2005

Optical response of polycrystalline mercuric iodide photoconductive detectors

Prashant Chegoor
University of South Florida

Optical Response of Polycrystalline Mercuric Iodide Photoconductive Detectors

by

Prashant Chegoor

A thesis submitted in partial fulfillment
of the requirements for the degree of
Master of Science in Electrical Engineering
Department of Electrical Engineering
College of Engineering
University of South Florida

Major Professor: Don L. Morel, Ph.D.
Christos S. Ferekides, Ph.D.
Yun. L. Chiou, Ph.D.

Date of Approval:
March 24, 2005

Keywords: HgI_2, Surface Recombination, Bulk Recombination,
Spectral Response, I-V Curves

ACKNOWLEDGMENTS

I would like to take this opportunity to express my sincere gratitude to my Major Professor, Dr Don Morel. He constantly stood as a source of Inspiration throughout this research. His keen Insight and valuable suggestions had motivated me through thick and thin in this research. Apart from this I personally have learnt a lot from him due to his high Integrity and composed nature. I would like to thank Dr. Christos Ferekides, a seasoned researcher in the field of Thin Film Solar cells, for all his valuable feedbacks during our research group meetings. I would like to thank Dr Y.L.Chiou for agreeing to be a part of my defense committee.

A word of appreciation also goes to my colleagues from the Thin Film Compound Semiconductor Lab at USF especially Vikram, Prince and Sridevi.It was indeed a wonderful experience working with them.My friends in USF and in India also deserve credit for their congeniality. Last but not least, I am always Indebted to my Parents who were the driving force behind all the earnest endeavors undertaken by me till now.

TABLE OF CONTENTS

LIST OF TABLES

LIST OF FIGURES

OPTICAL RESPONSE OF POLYCRYSTALLINE MERCURIC IODIDE PHOTOCONDUCTIVE DETECTORS

Prashant Chegoor

ABSTRACT

Mercuric Iodide in its tetragonal form has received a lot of attention for many years as a prospective room temperature X-ray and γ-ray detector. Its basic properties are well suited for this purpose. Its wide band gap of 2.1eV contributes to a high dark resistivity of 10^{12}ohm-cm or higher. A high atomic number of its constituent atoms (Hg-80, I -53) and a density of 6.3g/cm^3 result in its efficient interaction with incident X-ray or γ-ray radiation. Single crystalline mercuric iodide has been thoroughly studied and successfully utilized in commercial radiation detectors. But with the urgent need for large area ,low cost efficient X-ray detectors, focus has now shifted towards the development and understanding of the properties of thin film Polycrystalline Mercuric iodide detectors. Such detectors also have the advantage of being most suited for direct X-ray detection i.e. a direct conversion of incident X rays into electric signals which are then used to obtain an equivalent image in digital X-ray imaging. They also can be used in applications where a scintillator intermediate is used to generate visible light from incident high energy photons.

Therefore it is important to study their optical response in order to understand and evaluate their Optical Properties.

The present work focuses on obtaining the Optical response of the thin film Mercuric iodide photoconductive detectors .These films were grown on TEC-15 LOF glass with a Tin Oxide (SnO_2) coating on it, which acts as a growth surface for the films and also functions as the front contact of the detector. Palladium which is sputtered on top of this film acts as the back contact. There are a total of seven contacted devices on each film sample and each device has been tested for its optical response in terms of Spectral Response and I-V characteristics in both light and dark conditions. Results obtained have been tabulated, and some important samples have been analyzed. The aim in this research was to obtain films with high QE,low dark current and uniformity of the results for all devices on a sample.Typical values of high QE's obtained for the samples ranged from 0.3 - 0.4 with a bias of -50V applied to the front contact. The photocurrents corresponding to these QE's ranged from 2.83μA – 3.82μA as obtained from the spectral response data file. The dark currents that were measurable were typically below 50nA for the best sample.

CHAPTER 1

INTRODUCTION

Semiconductors are playing a vital role in influencing us by making our daily life more comfortable than before. Semiconductors are the backbone of many electronic devices that we use today. With the rapid developments in the Semiconductor Technology over the last fifty years, electronic devices have become smaller, faster and more reliable. Radiation detectors fabricated with Semiconductor materials is one such category of devices which has received a lot of attention with the rapid developments in the Semiconductor Technology.

Semiconductor Radiation Detectors operate on the basic principle that when radiation meeting certain requirements is incident on the device, a charge pulse of electrons and holes is created in the volume of the device by some interaction process which are then separated and made to flow in opposite direction by the application of an electric field, thus producing a current in the external circuit which can be detected. The amount of charge thus collected is a measure of the energy of radiation incident on the detector. Therefore there are many factors that have to be considered during detector operation such as nature of interaction of radiation with the semiconductor constituting the detector, the efficiency of the excitation process, the efficiency of

the charge collection process, the external circuit detecting the charge pulse and finally the background noise of the detector. The detector noise as well as the nature and efficiency of interaction between the particular radiation and the detector volume and the charge collection process will determine what materials may be employed to fabricate detectors for a specific purpose. For the Fabrication of room temperature X-ray and γ ray detectors the semiconductor material should satisfy the following requirements [1].

1) High Atomic number and Density for high photon absorption.
2) Large Band Gap for high resistivity and to minimize leakage currents at room temperature.
3) High Intrinsic Electron and Hole mobility life time products for efficient charge collection.
4) High purity, homogeneous , defect free material with acceptable cross-sectional area and thickness.

X-ray detectors are further divided into two groups known as Indirect and Direct detectors. Indirect Detectors are those in which the X-ray photons are first converted to visible photons by adopting a phosphor based scintillator and then these visible photons are converted into an electrical signal by means of photodiode arrays. For Digital X ray imaging this signal is transformed into an equivalent image by sensing it with an electronic readout mechanism followed by a analog to digital conversion to obtain the digital image [2]. Obviously this two step process suffers from many disadvantages including low energy transfer efficiency and low energy resolution [3]. In contrast, Direct Detectors offer a one

step conversion of X-ray Photons into Electrical signals by means of a X-ray photoconductive detector which can then be transformed into an image by the same process as mentioned above. Thus this results in higher QE and resolution for this detector. In this context polycrystalline Mercuric Iodide detectors show promise as Direct X-ray detectors in digital radiography.Polycrystalline Mercuric Iodide also finds applications in indirect detection wherein a scintillator intermediate is used to generate visible photons from incident high energy photons. The present work therefore deals with polycrystalline HgI_2 photoconductive detectors with emphasis only on their Optical response. As shall be discussed later, Photoconductive detectors are the simplest subdivision of the Photodetectors consisting of a semiconductor material sandwiched between two metal contacts. Before proceeding further it is worthwhile to compare some of the properties of Polycrystalline HgI_2 in comparison to the other semiconductors used for direct detection .Table 1.1 summarizes these properties.

From the table it can be seen that the value of Atomic Number (Z) for HgI_2 is high enough for the efficient absorption of X-rays since the predominant photoelectric absorption process for X-rays in materials is proportional to the Atomic number, Z .The X-ray energy required to generate an electron – hole pair for HgI_2 is also low which results in high signal strength and resolution. The high mobility- lifetime product in HgI_2 results in greater distance traversed by the generated charges and thus leads to better charge collection and high sensitivity. The lower voltage operation allows low voltage electronic design.

Table 1.1 Comparisons of Some X-ray Sensitive Semiconductor Materials for Direct Detection [4]

	Poly-HgI_2	Poly-PbI_2	a-Se	Poly CdZnTe	Comments
Atomic Number (Z)	80,53	82,53	34	48,30,52	Absorption increases with Z
Energy Band Gap (Eg) eV	2.1	2.3	2.2	1.5	Broader gap- lower dark current
Charge Pair Energy Formation (W) eV	5.5	6.6	50 (effective)	4.5	Lower W - higher gain
Mobility Life-time Product ($\mu\tau$) cm^2/V	10^{-5}	(h) $1.8X10^{-6}$ (e) $7X10^{-8}$	$10^{-6} - 10^{-5}$	10^{-5}	Higher $\mu\tau$ - better charge collection
Operational Electric Field (E) V/cm	10^4	10^5	10^5	10^5	Lower E - reduced electrical breakthrough
Processing Temperature (°C)	100	200	400	600	Lower temperature – simpler process

Finally this chapter ends with a brief overview of some applications of HgI_2 detectors [1].

1) In medical diagnostic applications especially for digital mammography.

2) In non destructive evaluation of materials during security checks at ports.

3) In geological and marine explorations of minerals.

4) In environment pollution monitoring.

5) In x-ray analysis of biological samples and astronomical observations.

The following chapter discusses some of the Semiconductor processes relevant to study of Photoconductive detectors. An understanding of these processes is needed to examine the operation and performance of Photoconductive detectors.

CHAPTER 2

SEMICONDUCTOR PROCESSES

2.1 Introduction

The variability of the Electrical properties of Semiconductors makes them the perfect choice for fabricating electronic devices. Their electrical conductivities lie between those of Metals and Insulators. Their electrical conductivity can be varied drastically by means of change in temperature, Optical excitation and by the incorporation of impurities in the material by a process named as Doping. Every Solid be it Metal, Insulator and Semiconductor has its own characteristic energy band structure. All band structures are characterized by an upper band of allowed states called the Conduction band and a band of allowed states below this band called the Valence band which is mostly filled with electrons. The valence band and the conduction band may or may not be separated by a forbidden gap of allowed states called the Band gap. The distribution of states in each of these bands according to the energy is given by the Density of States function ,denoted by $g_c(E)$ and $g_v(E)$ for the conduction and valence band respectively.It thus represents the number of states that are available at an energy E. The probability that an available state at an energy E is occupied by an electron is given by the probability distribution function called

Fermi Function, denoted by f(E).Mathematically the Fermi function can be expressed at thermal equilibrium as,

$$f(E) = \frac{1}{1 + \exp(E - E_F)/kT}$$

Where E_F = Fermi energy or Fermi Level in eV

k = Boltzmann constant in eV/K

T = Temperature in K

At a temperature of 0K all available energy states below the Fermi energy level are completely filled. The probability that a state at a energy E is not occupied is given by 1-f(E). The products $g_c(E).f(E)$ and $g_v(E).(1-f(E))$ therefore represent the distribution of electrons and holes in the conduction band and valence band respectively.

In metals the conduction and the valence band typically overlap or the conduction band is only partially filled. This leads to the intermixing of electrons and empty energy states which leads to high conductivity of metals in the presence of an electric field.In Insulators the magnitude of energy gap is large for e.g. in Diamond an insulator it is about 5eV.At 0 K the valence band in diamond is completely filled whereas the conduction band is empty. Due to non availability of empty states in the valence band there can be no charge transport within the valence band and due to the absence of electrons in the conduction

band there can be no charge transport there either. Therefore insulators possess high resistivity.In semiconductors the band gap is typically much lower (0.1eV-3.0eV) than in insulators which allows electrons to be easily excited from the valence band to the conduction band by means of supplying thermal or optical energy. Such excitation is difficult to achieve in Insulators. In this aspect Semiconductors differ from Insulators even though their band structure at 0 K is similar to that of the Insulators with a completely filled Valence band and an empty Conduction band.

2.2 Carrier Transport

Electrical conduction in semiconductors is due to the movement of both the electrons and the holes in the conduction and the valence bands respectively. For this to take place the first requirement is that there should be a partially filled band since a completely filled band and a completely empty band will not conduct. The second requirement is that the carrier motion should have a net direction and the two mechanisms by which such a directional motion is possible are known as Drift and Diffusion[5] .Normally under thermal equilibrium mobile electrons in the conduction band and holes in the valence band are in random thermal motion resulting in zero net current .The randomness in the motion is caused by carrier scattering mechanisms such as phonon (lattice)scattering, ionized impurity scattering ,neutral impurity atom scattering, carrier-carrier scattering, crystal defects scattering etc. Now when a external field (ε) is applied across the semiconductor as shown in Fig.2.1(a), the resulting

force on the carriers tends to accelerate the +q charged holes in the direction of electric field and the –q charged electrons opposite to the direction of electric field, where q stands for the electronic charge. But due to scattering caused by the above mentioned mechanisms the motion of carriers for eg holes, though in the direction of the field occurs in a disjointed fashion involving repeated periods of accelerations and subsequent decelerations as shown in Fig.2.1(b) .Thus the microscopic motion analysis looks somewhat complicated but measurable quantities being macroscopic in nature reflect the average or overall motion of the carriers. When such an average is carried out over all the carriers the resultant motion can be visualized on a macroscopic scale as in Fig 2.1(c) [6].The motion of each carrier now can be described in terms of a constant velocity v_d called drift velocity . Such a mechanism of charged particle motion in presence of an applied field is known as Drift.

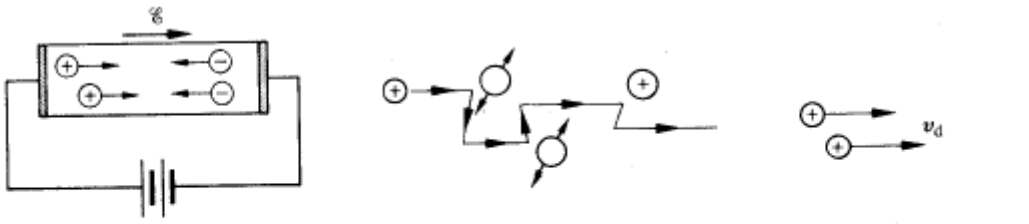

(a)Motion of holes in a Semiconductor bar (b) Motion on a microscopic scale (c) Motion on a macroscopic scale

Figure 2.1 Visualization of Carrier Drift [6]

It is to be noted that above drifting motion is actually superimposed on the always present thermal motion of the carriers which being completely random in nature averages out to zero on a macroscopic scale and thus does not contribute to carrier transport and is therefore neglected. The measured drift

velocity (v_d) in semiconductors for low to moderate field values of electric field (ε) is directly proportional to the applied electric field. The constant of proportionality is termed as Mobility (μ).This is an important parameter which plays a key role in characterizing the performance of a device.It can be interpretated as the ease with which a carrier can drift within a semiconductor crystal. It is a function of the amount of carrier scattering, temperature and the doping of the semiconductor. At higher electric fields the drift velocity tends to saturate thereby becoming field independent [7].

The second mechanism called Diffusion arises when there is a non uniform density of carriers – electrons and holes. Thus in the absence of any other processes such as drift ,the carriers will diffuse from a region of high density to a region of low density.Also thermal motion not interparticle repulsion is the enabling action behind the diffusion process. Fig .2.2 (a) [5] shows a 2-D representation of the Diffusion process on a microscopic scale.Under thermal equilibrium each carrier has equal probability of moving in either the –x or +x direction.The graph shows the carrier concentration vs. distance at various instances of time t such that $t_1<t_2<t_3$.However if there is a concentration gradient there will be a net of flow of carriers from a high concentration to a lower concentration as shown if Fig 2.2(b) [6].Here $J_{P \mid diff}$ and $J_{N \mid diff}$ refer to hole and electron diffusion current densities respectively.

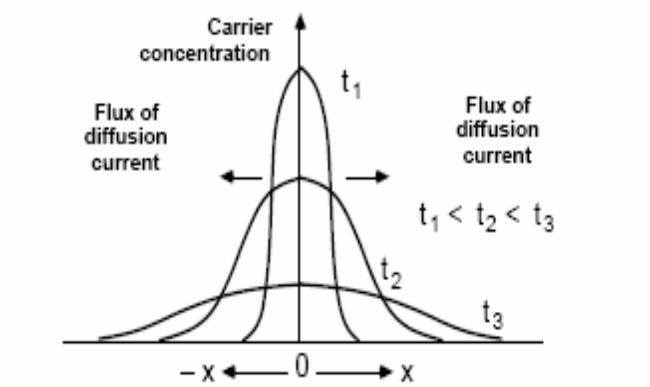

(a)

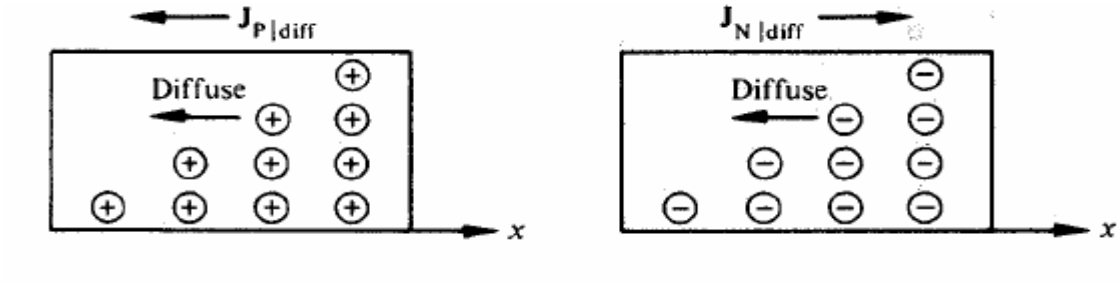

(b)

Figure 2.2 Visualization of the Carrier Diffusion Process [5, 6]

Having discussed about the carrier motion processes in the semiconductors it is now necessary to explain certain concepts related to carrier generation and recombination processes which are important to the subject of the present work.

2.3 Carrier Recombination and Generation Processes

When a semiconductor is disturbed from the equilibrium state, an excess or deficit in the carrier concentrations relative to their equilibrium values is invariably created inside the semiconductor. In this situation there comes into existence the process of carrier recombination and generation which tries to stabilize the carrier excess or deficit if the perturbation is still maintained and if not the process tries to eliminate such an excess or deficit of carriers. Since one often encounters non equilibrium conditions during device operation this process therefore plays a vital role in shaping the characteristics exhibited by a device. Broadly speaking a Recombination process is defined as one which destroys or annihilates electrons and holes. Generation on the other is a mechanism by which electrons and holes are created. Also unlike Drift and Diffusion mechanisms the terms Recombination and Generation do not refer to a single process but they are collective names for a group of similar processes which means that carriers can be destroyed and created within the semiconductor in a number of ways. It is therefore convenient to denote these processes as R-G processes. The most important of these processes are shown in Fig 2.3 [6]. A brief explanation of each process shall follow thereafter.

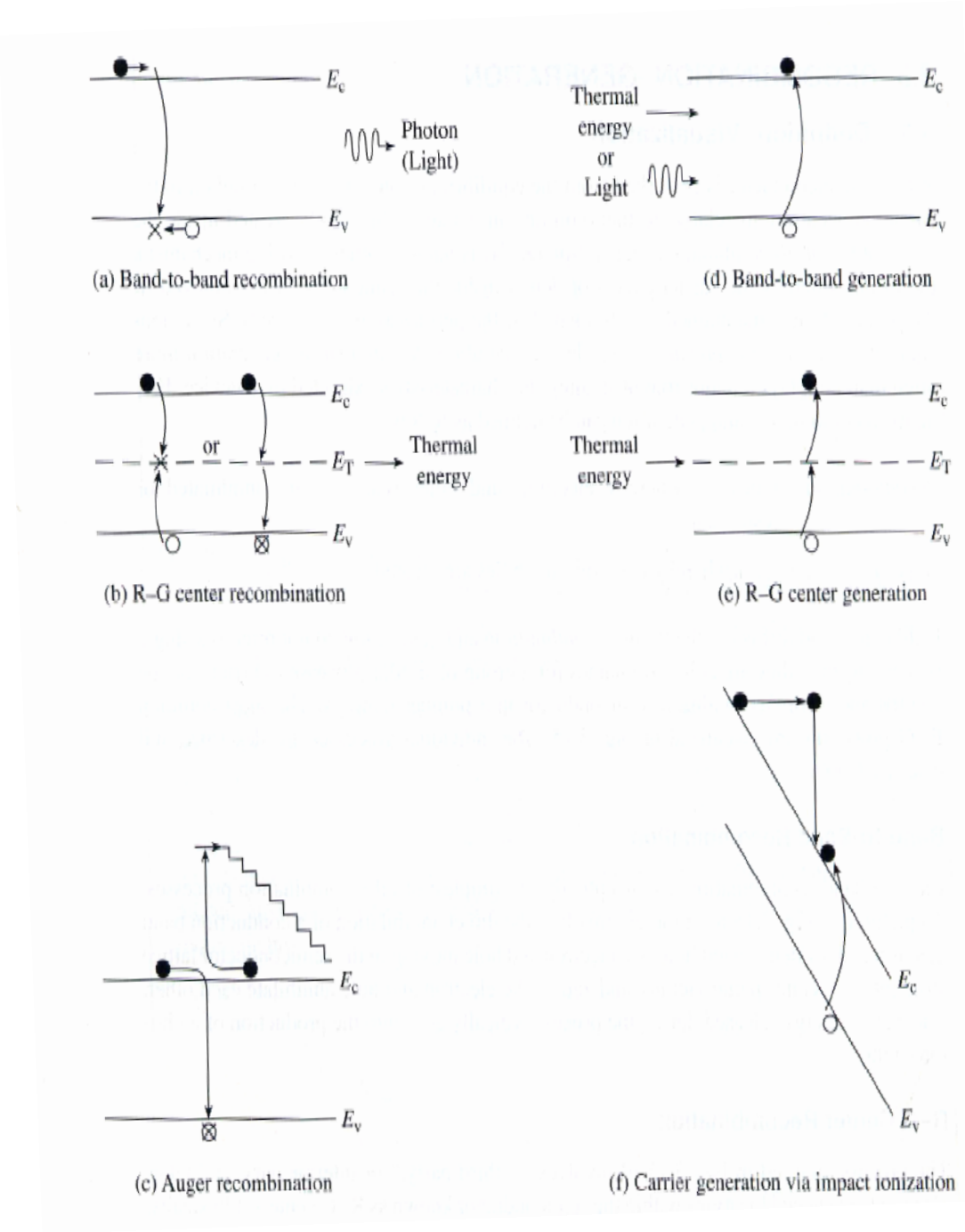

Figure 2.3 Energy Band Visualization of Bulk Recombination and Generation Processes [6]

2.3.1 Recombination Processes

2.3.1.1 Band-to- Band Recombination

This is conceptually the simplest of all recombination processes. As shown in Fig. 2.3(a) it merely involves the direct annihilation of a conduction band electron and a valence band hole. When the electron and hole moving in the semiconductor lattice stray into the same spatial vicinity they annihilate each other and the excess energy released during this process typically goes into the production of a photon of energy approximately equal to the band gap energy. This recombination is also called direct thermal recombination.

2.3.1.2 R-G Center Recombination

This type of process usually plays a central role and often dominates other recombination and generation processes. This process is pictured in Fig. 2.3(b) involves a third party or a intermediary and takes place only at special locations within the semiconductors known as R-G centers. R-G centers are lattice defects or special impurity atoms such as gold in Si.Even in semiconductors of highest available purity, lattice defects and unintentional impurities are always present. The R-G center concentration however is normally very low compared to the acceptor and donor concentration in device quality materials.The most important property of these R-G centers is the introduction of allowed energy levels generally near the center of band gap.It can be shown that the most efficient R-G centers are those that

introduce energy levels at the mid band gap region [8]. Actual semiconductors can have a number of deep level R-G centers but the process is usually dominated by only one type of R-G center. As shown in Fig.2.3(b) first one type of carrier and then the other type of carrier is attracted to the R-G center. Thus the capture of an electron and hole at the same site leads to the annihilation of the electron–hole pair. This can also be equivalently visualized as the transition of a carrier first to the R-G center and then an annihilating transition to the opposite carrier band. R-G center recombination also called indirect thermal recombination is characteristically non-radiative. Thermal energy (heat) is released during the process or equivalently lattice vibrations also called phonons are produced. An important clarification has to be made at this juncture regarding the difference between the terms Trap and R-G center.Broadly speaking the chemical impurities and lattice defects introduce localized allowed energy states in the band gap region.A localized energy state can generally be effective in only one way either as a Trap or a R-G center .If a carrier that is attracted to a localized state is re-excited back after a certain time to its corresponding energy band before it recombines with an opposite carrier then the localized state is said to be acting as a Trap for that carrier. If the same state however assists in recombination then it is termed as a R-G center.Generally energy states introduced by impurities and defects which are close to either conduction or valence band edges act as effective electron and hole traps respectively.Charge carrier trapping in many devices can play a pivotal role in affecting their performance.The time that a charge

carrier is free so as to contribute to conductivity is called free life time of the charge. It is denoted by τ .It is the time that an excited electron spends in the conduction band or the time that an excited hole spends in the valence band. The time spent by the electron or hole in the trap is not included in the free life time. It is represented by τ_n and τ_p for electron and hole respectively.For a direct band to band recombination both of these lifetimes are equal because annihilation of both electron and hole occurs at the same time but for R-G center recombination this may not be true.The free lifetime of a charge carrier can be [9] :

(a) Terminated by recombination, or if the carriers are extracted from the semiconductor without being replenished from the opposite electrode.

(b) Interrupted if the carrier is trapped, to be resumed after the carrier is freed from the trap.

(c) Undisturbed if the carrier is extracted from the semiconductor by the applied electric field at the same time as an identical carrier is injected into the semiconductor from the opposite electrode.

The free life time of a carrier is inversely proportional to the product of number of R-G centers per cm^3 and the capture cross section (σ cm^{-2}) of the R-G center.The capture cross section measures the effectivenesss of an R-G center or a trap to capture a free carrier. Each localized state in the band gap region has two capture cross sections one for the electron and one for the hole. For a

energy state in the band gap acting as a true R-G center $\sigma_n=\sigma_p$.For a state acting as True Hole trap $\sigma_p >> \sigma_n$ and for true electron trap $\sigma_n >> \sigma_p$ [5].

2.3.1.3 Auger Recombination

In the Auger process shown in Fig. 2.3(c) a band to band to recombination occurs simultaneously with the collision between two like carriers.The energy released by the recombination is transferred during the collision to the surviving carrier.This highly energetic carrier subsequently "thermalizes "- loses energy in small steps through heat producing collisions with the semiconductor lattice as shown in the picture.

2.3.2 Generation Processes

All of the above recombination processes can be reversed so as to generate free carriers. Fig. 2.3(d) shows the band to band generation where an electron is excited directly from the valence band to the conduction band. Either thermal energy or Light energy can be used to provide the energy required for band to band transition. If thermal energy is used then the process is termed as Direct Thermal generation. If externally introduced light is absorbed then the process is called Photogeneration .The thermally assisted generation of carriers with R-G centers acting as intermediaries is envisioned in Fig 2.3(e).The photoemission of carriers from band gap centers also can also be pictured but it is typically a rather improbable process. Finally impact ionization, the inverse of Auger recombination is shown in Fig. 2.3(e).In this process an electron –hole pair

is formed due to the energy released when a highly energetic electron collides with the crystal lattice. Such a generation of charges usually occurs in high Electric field regions of the device [6].

The recombination and generation processes discussed above occur at all times in the semiconductors-they even occur when under thermal equilibrium.Under thermal equilibrium conditions however each fundamental process and its inverse must self balance independent of any other process occurring inside the semiconductor[10].Generally one is concerned with only the process which is dominant among all other processes occurring in a semiconductor under certain conditions.Not all processes occur at the same rate under certain conditions. In order to get a better understanding of the processes which would dominate in a semiconductor it is essential that one visualize these processes by means of changes in crystal momentum in addition to energy change. This is because in any R-G process both energy and crystal momentum has to be conserved. Crystal momentum (ħk) related aspects of R-G processes are conveniently discussed by means of Energy – Momentum (E-k) plots. Semiconductors can be classified as Direct and Indirect Semiconductors on the basis of these E-k plots.

2.4 Direct and Indirect Semiconductors

The difference between the two types of semiconductors is evident in the E-k plots of Fig.2.4 [6]. In a Direct semiconductor both the minimum energy of the

conduction band and the maximum energy of the valence band occur at k =0.In an Indirect semiconductor the conduction band is displaced to k≠0.Here E_C and E_V refer to conduction band minimum and valence band maximum respectively.

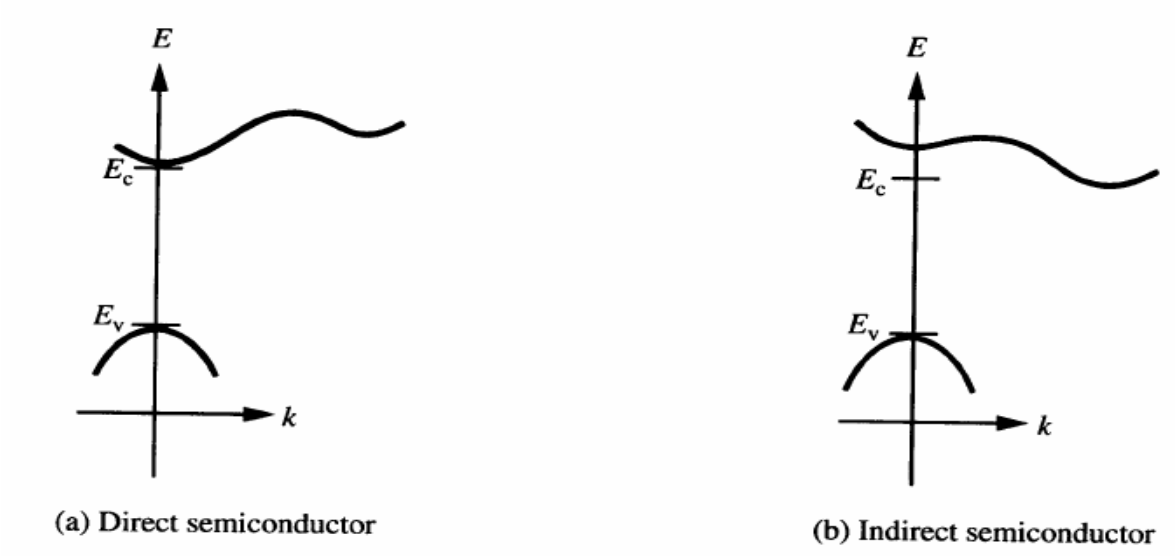

Figure 2.4 The Two Different Types of Semiconductors [6]

In order to visualize a R-G process using a E-k plot an understanding of the nature of transitions associated with the absorption and emission of photons (light) and lattice vibration quanta called phonons is necessary.Photons, being massless identities,carry very little momentum and a photon assisted transition is essentially vertical on the E-k plot.On the other hand the thermal energy associated with lattice vibrations (phonons) is very small but the phonon momentum is comparatively large.Thus on the E-k plot the phonon assisted transition is essentially horizontal.Also it has to be mentioned here that electrons and holes usually occupy states close to E_C minimum and E_V maximum respectively[6].Now as shown in Fig.2.5 (a), a band to band recombination in a

direct semiconductor effectively proceeds because the k values of all the electrons and holes are bunched at k=0, leading to a low change in momentum for the recombination process. Conservation of both energy and momentum is readily met by emission of a photon as shown. A band to band to recombination in an indirect semiconductor as visualized in Fig.2.5 (b) requires a large change in momentum.Consequently the emission of a photon must be accompanied by a emission or absorption of phonons.The rather involved nature of such a band to band recombination in indirect semiconductors leads to a vastly diminished rate.In an indirect semiconductor an electron in the conduction band minimum at k≠0 cannot recombine with a hole at k=0 in the valence band maximum unless a phonon of the right energy and momentum is available.Both phonon emission and phonon absorption can assist the downward transition.In order for the right phonon collision to occur the dwell time of the electron in the conduction band increases..It therefore implies that the electron will more likely recombine non radiatively with a hole through R-G centers which are always present due to impurities and lattice defects in the crystal.Thus Band to Band recombination is in fact totally negligible compared to R-G center recombination in indirect semiconductors. Therefore the probability of radiative recombination in a Direct semiconductor is very high compared to radiative recombination in indirect semiconductors. The non radiative competing processes reduce the probability of radiative recombination in indirect band gap materials.Similarily Band to Band absorption of light by an electron in an Indirect Semiconductor also involves a

phonon for momentum conservation and the probability of this happening is thus reduced when compared to such an absorption in a Direct semiconductor.

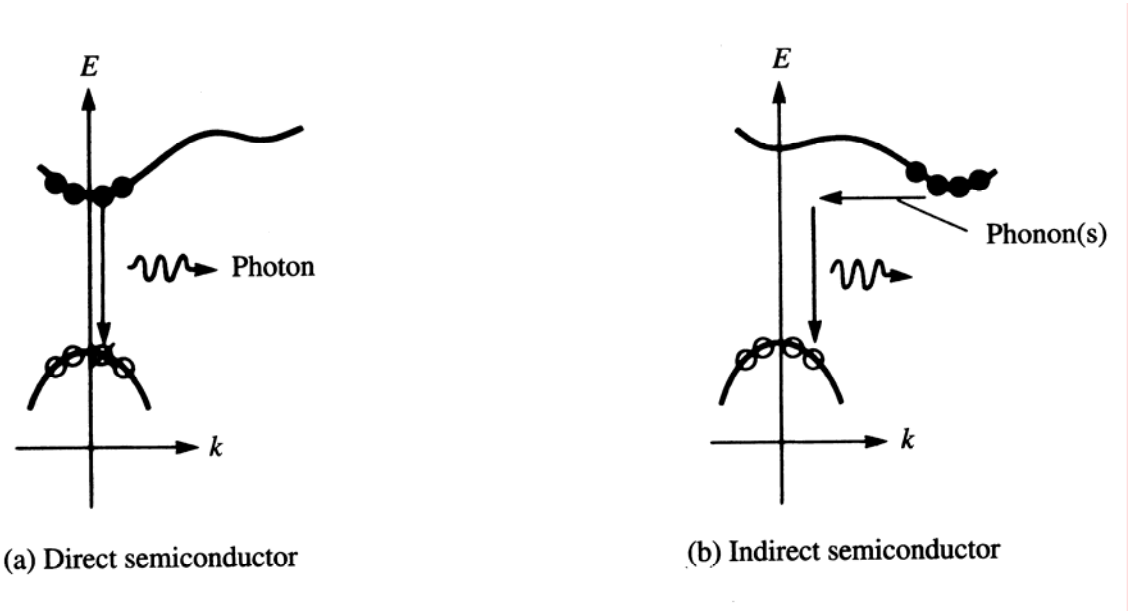

Figure 2.5 E-k plots for Visualizations of Recombination (band to band) in Direct and Indirect Semiconductors [6]

The Recombination -Generation mechanisms discussed so far take place in the bulk of the semiconductor as opposed to Surface Recombination – Generation taking place near the vicinity of Semiconductor surface via interaction with interfacial traps. Though the former is important, the latter is as important and many times more important than the former.Since the properties of many photodetectors are affected by generation and recombination at the surface, a brief discussion is in order.

2.5 Surface Recombination-Generation

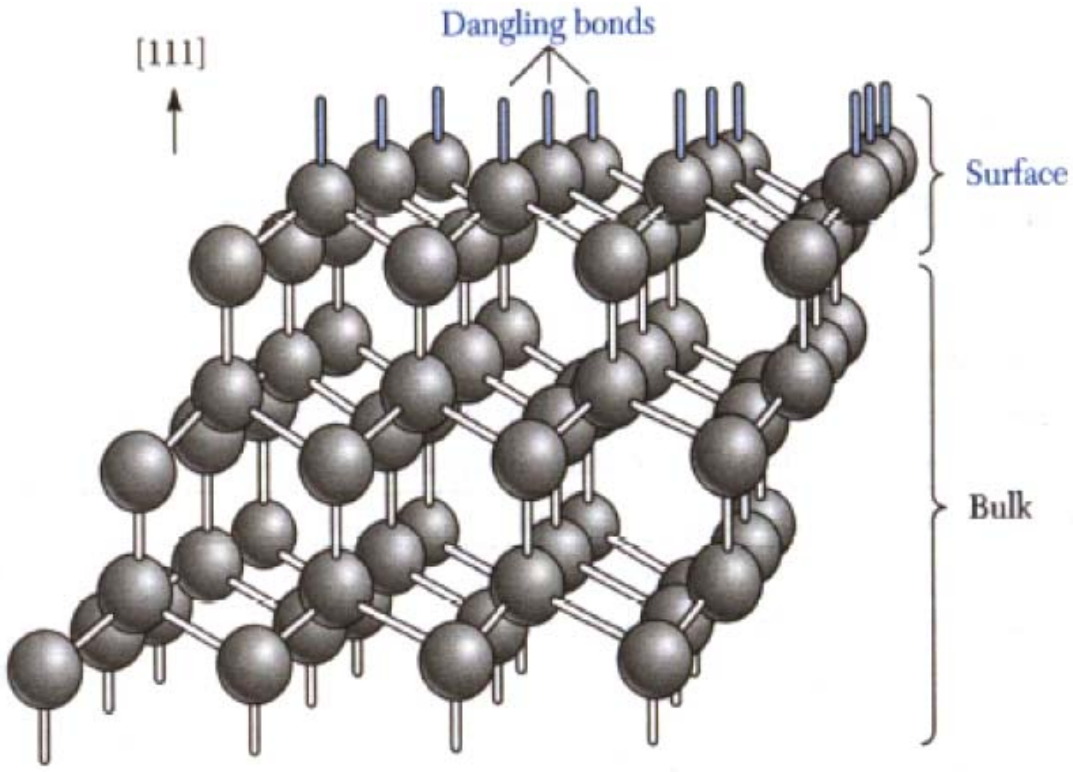

Figure 2.6 Abrupt Termination of the Semiconductor Lattice Structure at the Surface [11]

As shown in the Fig.2.6 there is abrupt termination of the lattice structure at the semiconductor surface. The surface usually consists of dangling bonds or bonds that are satisfied by atoms other than the host atoms. The presence of dangling bonds, surface imperfections, foreign atoms on the surface, etc result in the introduction of a large number (more than in the bulk) of localized R-G centers at the surface region called the surface centers or states.Unlike the bulk R-G centers , however ,the surface centers are found to be continuously distributed in energy throughout the semiconductor band gap .This is pictured in

Fig. 2.7 . The same fundamental processes that occur in the bulk also occur at the semiconductor surface.Electrons and holes can be captured at these surface centers and also can be emitted from theses surface centers. Though seemingly possible from the energy band diagram the additional transitions occurring between surface centers of different energies is extremely unlikely because of the spread out or spatially isolated nature of centers on the surface plane. This is shown in Fig. 2.7(c).

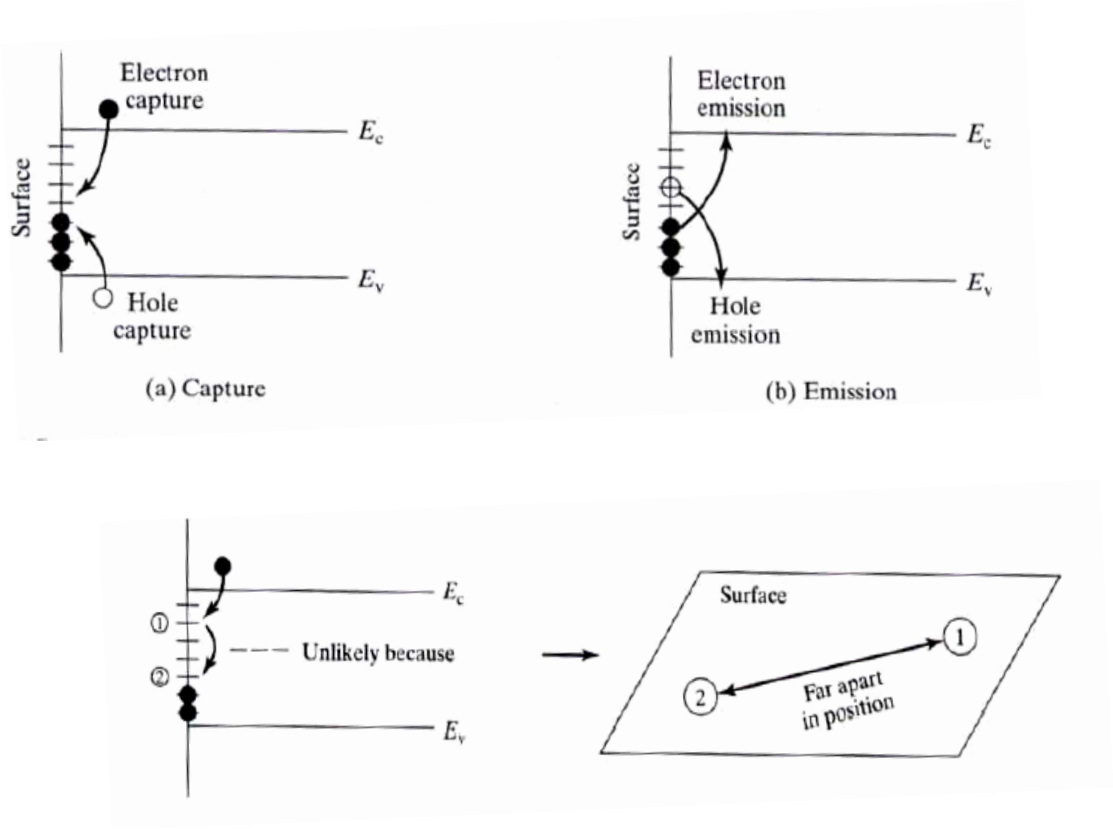

(c)

Figure 2.7 Processes at the Semiconductor Surface

The parameter responsible for gauging the surface recombination and surface generation rate is the Surface recombination and surface generation

velocity respectively. Both have the units of velocity (cm/sec).The higher the surface recombination (generation) velocity the greater the surface recombination (generation). Both depend on the state of the semiconductor surface whether accumulated, depleted or inverted .Surface recombination(generation) velocity is also proportional to the product of the total surface centers per unit area (N_{ST}) and the capture cross section of the surface center [10].

With the introduction of various processes in a semiconductor which influence carrier motion and their numbers it is now time to analyze one fundamental process of carrier generation relevant to the present work in greater detail namely the process of Photogeneration in semiconductors and also the operation of Photoconductive detectors. This shall be the subject of discussion in the next chapter.

CHAPTER 3

PHOTOGENERATION AND PHOTOCONDUCTIVE DETECTORS

3.1 Photogeneration

The first stage in the operation of any photodetector is the absorption of light quanta of appropriate energy resulting in the generation of free charge carriers.This is the basic principle in converting any electromagnetic radiation energy into electrical energy. There are several processes by which photons (light) are absorbed in matter [11] of which the process of interest for the present study is the Photogeneration.Simply stated it is the process of exciting an electron from the valence band to conduction band leading to formation of free electron in the conduction band and free hole in the valence band by means of absorption of a photon.The required photon energy for photogeneration is thus atleast equal to the band gap energy.As previously discussed this is a special case of Band to Band transition assisted by the absorption of light. Such a band to band absorption process is also called the fundamental (absorption) process. Independent of the process of absorption, the Intensity (Optical power per unit area) of the light decreases with distance inside a Semiconductor according to the well known law known as the Beer's Law as illustrared in Fig.3.1.The plot shows the exponential decay of intensity of photons with respect to the distance (x direction) in the material .Here the intensity of the incident photons is I_o ,I_t is the

intensity of transmitted photons at the distance t ,where t is the thickness of the Semiconductor. Here it is assumed that photons do not undergo any kind reflection at the front and back surfaces of the semiconductor.

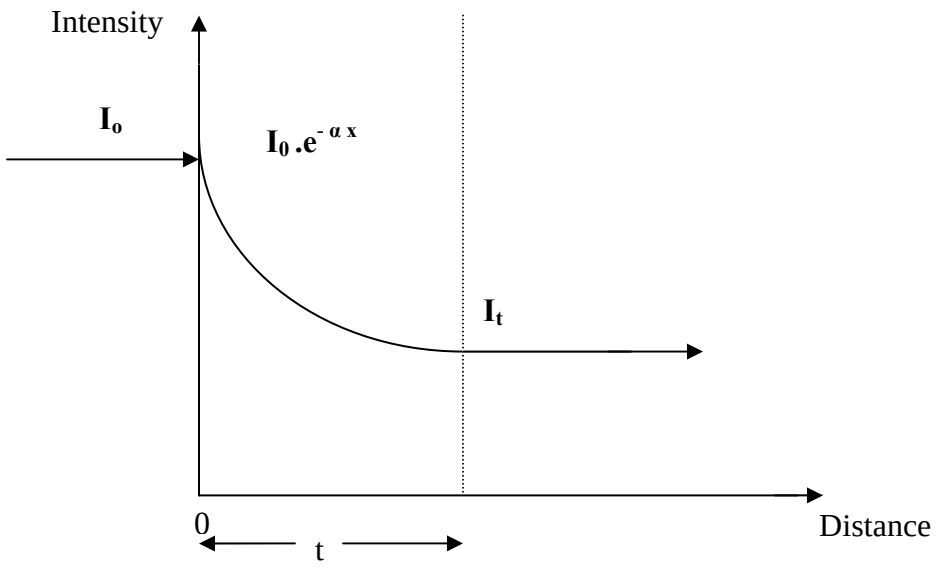

Figure 3.1 Exponential Decay of Photon Intensity Inside a Semiconductor

The Beer's Law in the form of an equation can be expressed as

$$I_{(x)} = I_0 .e^{- \alpha x} \quad ,$$

$I_{(x)}$ is the intensity at a distance x in the Semiconductor.

The quantity of interest in this equation is α (cm^{-1}), known as the absorption coefficient of the semiconductor. The degree of absorption of light in a semiconductor is quantified by its absorption coefficient. It is a strong function of material and the wavelength of incident photons.It generally varies with different

absorption processes.For the fundamental absorption process discussed at the beginning of this section the absorption coefficient increases rapidly with the photon energy above the band gap energy of the semiconductor under consideration,and for Direct Semiconductors the absorption coefficient is found to be greater than in Indirect Semiconductors.This suggests stronger absorption of light in Direct Semiconductors when compared to Indirect semiconductors the reasons for which have already been discussed in the previous chapter.The significance of the absorption coefficient also lies in the fact that its reciprocal represents the distance over which the Intensity of photons falls to a value of 1/e. This distance given by $x=1/\alpha$ is called the penetration or absorption depth.For complete absorption of light of appropriate wavelength the thickness of the semiconductor should be greater than the absorption depth. The energy of each photon is given by the relation,

$$E_{photon} = hc / \lambda,$$

Where h is the Planck's constant in eV-s

c is the speed of light in Vacuum in m/s

λ is the wavelength of light in m

Thus based upon the above facts lower wavelength light consisting of higher energy photons is absorbed strongly at the front surface of the semiconductor region compared to longer wavelength light .When the energy of each photon is below the band gap of the semiconductor then the absorption is negligible and than the semiconductor is said to be transparent to such light. This is possible

only if the semiconductor is assumed to be free of impurities and defects which would give rise to energy states in the band gap region and consequently absorption of light of energy below band gap is also possible.Such an absorption from the impurity levels in the band gap is known as impurity absorption. Of course there are other absorption processes giving rise to absorption below the band gap energy which shall not be discussed here.

3.2 Photoconductor

The photoconductor is the simplest photodetector consisting of a slab of semiconductor (in bulk or thin-film form) with two metallic contacts or electrodes fixed at the opposite ends and across which a voltage is applied.The voltage applied is a dc voltage in the present case. Its operation is based on Photoconductivity. Photoconductivity is the property of a Semiconductor by which its bulk conductivity increases due to absorption of light. Generally in a semiconductor under thermal equilibrium there is a balance between thermally generated free carriers and their recombination which determines their number. Additional free carriers can be produced by means of absorption of light resulting in increased conductivity which persists as long as the additional carriers recombine or until they are extracted out at the electrode without being replenished from the opposite electrode .Based on the light absorption process photoconductors are divided into two types namely Intrinsic and Extrinsic Photoconductors.In Intrinsic photoconductors the light is absorbed by the process of photogeneration involving creation of free carriers by band to band

transition.A photon of energy equal to or greater than the energy gap is typically required.In an extrinsic photoconductor light is absorbed by filled impurity states in the band gap region resulting in production of free carriers.Focus here will be only on the Intrinsic photoconductor. Some terms related to photoconductors can be defined as below.

3.2.1 Quantum Efficiency (QE)

There are two types of quantum efficiency Internal and External .Internal quantum efficiency is the ratio of number of electron –hole pairs which are created per second and detected to the number of photons absorbed per second in the photoconductor.External quantum efficiency on the other hand is the ratio of the number of electron-hole pairs which are created per second and detected to the number of photons per second impinging on the semiconductor surface.Thus the external quantum efficiency does not take into account the photons lost due to reflection at the surface or transmission.Consequently Internal quantum efficiency is higher than External quantum efficiency. The maximum value of quantum efficiency can be 1. QE is a function of wavelength.

3.2.2 Gain

Before recombination occurs the Gain in a Photoconductor is defined as follows:

$$G = \frac{\text{(distance traversed by a electron) + (distance traversed by a hole)}}{\text{Distance between the electrodes}}$$

Normally when a photon is absorbed in a photoconductor an electron hole pair is created and if both of them reach their respective electrodes, then the photon is said to detected. The Gain in this case is 1.This is usually the case when the contacts to the semiconductor are of blocking nature which do not allow carriers to enter the photoconductor from the external circuit .Thus when an excited carrier exits the photoconductor from one electrode a similar carrier will not enter the photoconductor from the opposite electrode to maintain charge neutrality.But in the case of Ohmic contacts which allow carriers to flow in either direction with ease the charge neutrality condition is satisfied and therefore it is possible for an excited carrier usually the electron(as its mobility is higher than that of hole) to reach its electrode sooner than the hole and therefore due to charge neutrality the external circuit provides another electron to the photoconductor which once again moves faster than the hole reaching its electrode before the hole reaches its electrode.This process will continue until the electron recombines with the hole.Thus it is possible for the electron to traverse the distance between the electrodes more than once.Therefore the gain of the photoconductor is more than 1 in this case [9].Of course for this to happen the free lifetime of electron must be greater than its transit time(defined as the time time taken by the electron to travel the distance between the electrodes).

3.2.3 Photocurrent

The current due to flow of excess photogenerated carriers in the presence of an applied field is called is called Photocurrent.An expression for photocurrent in a photoconductor can be written as follows :

$$I_{ph} = e.G.\ F$$

where, e is the electronic charge,G is photoconductor gain and F is the rate at which the electron hole pairs are created in the photoconductor.It can be shown that G is proportional to the sum of the mobility-lifetime products of electron and hole [9].Therefore higher values of these products result in greater gain and consequently higher photocurrent.

3.2.4 Dark Current

Basically the dark current refers to the current flowing through the photoconductor when it is not illuminated.This current is mainly due to the flow of thermally generated carriers in the photoconductor.In some cases these carriers are higher than those excited by light and therefore this affects the performance of the photoconductor by causing rapid fluctuations in the output current which is a sum of both the photocurrent and dark current. Therefore. materials with a high band gap must be chosen to minimize the effect of the dark currents.

3.2.5 Spectral Response

A given photoconductor can be generally characterized by studying its Spectral response, which is plot of its External quantum efficiency(a function of wavelength) versus the wavelength of light.In the present work the Optical response of the Mercuric iodide Photoconductive detectors is analyzed by its Spectral response.

Photoconductivity is one of a few topics where the experimental setup, contact configuration, preparation of the sample and sample thickness all play a very vital role in the output and the analysis of the results.Two most commonly used configurations for photoconductor characterizations are shown in Fig.3.2. Fig 3.2(a) shows a configuration in which the device is illuminated along the direction of electric field through a transparent contact. Also shown here is the negative bias applied to the illuminated contact. Fig. 3.2 (b) shows a configuration in which the device is illuminated perpendicular to the direction of electric field in the photoconductor.

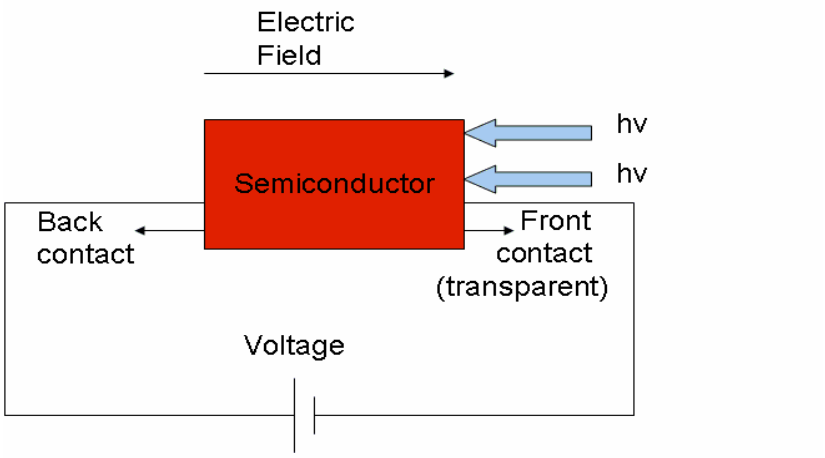

(a)

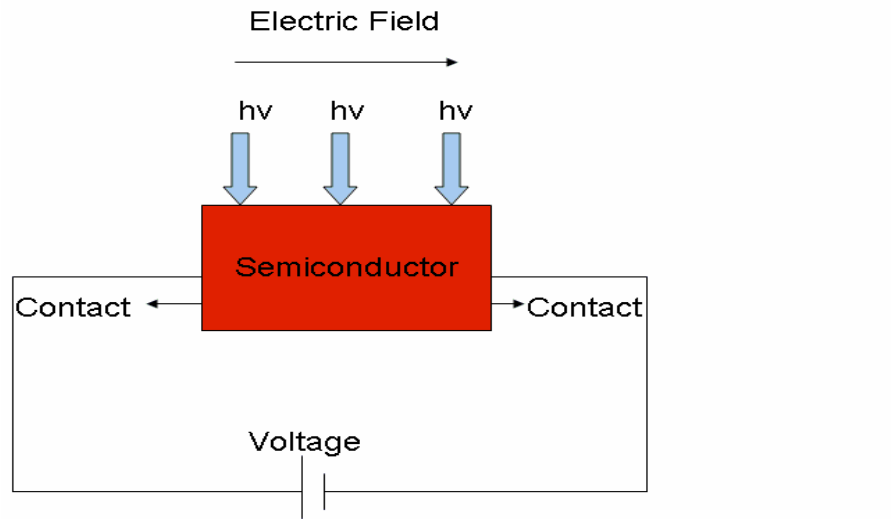

(b)

Figure 3.2 Different Experimental Configurations of a Photoconductor

The configuration of Fig 3.2(a) is used to obtain the Spectral response I-V curves for Thin Film Polycrystalline Mercuric Iodide photoconductive detectors in this work.

The above discussion on photoconductivity thus outlines some of its salient features and it is important to mention here that the photoconduction process involves generation, recombination and the transport of carriers to the electrodes. It is thus a complex process in which many vitals issues relating to above mechanisms have to studied. Inspite of this complexity the photoconduction process provides valuable information about physical properties of materials and thus offers application in photodetection and radiation measurements.Recent advances in thin film technology particularly in excellent quality crystal growth have given a new dimension to the field of photoconductors and now quantum well and superlattice photodetectors are a reality [13].

The next chapter addresses some of the important properties and issues of Mercuric Iodide material in relation to its use as detectors and investigated in some of the technical papers on this subject.

CHAPTER 4

MERCURIC IODIDE

4.1 Literature Review

Mercuric Iodide was one of the earliest materials to be investigated for photoconductivity. In 1903 it was shown that HgI_2 could be used with gelatin to form a photographic emulsion .Other workers thereafter studied the spectral response and photoconductivity mechanism in HgI_2 .The photoelectric properties of HgI_2 were extensively studied by Bube [14] both in its red phase (α-HgI_2) and on phase transformation to yellow (β- HgI_2) phase. HgI_2 crystallizes in the red tetragonal structure (α-HgI_2),which undergoes a phase transformation to yellow orthorhombic (β- HgI_2) form at 400 ^{o}K.Research carried out on the orthorhombic form of HgI_2 revealed that its photosensitivity was about 0.1% of that of the red tetragonal HgI_2[14,24] .Therefore the tetragonal form of HgI_2 is best suited for X-ray and gamma ray detector fabrication. The Crystal growth techniques, Electrical and Optical properties of HgI_2 have been extensively studied with respect to their radiation detection applications [1] and HgI_2 has proved to be an excellent material for the fabrication of Room temperature X-ray and gamma ray detectors. HgI_2 has a band gap of 2.1eV at room temperature and it has a small temperature coefficient of approximately 10^{-4}eV per kelvin which results in a small thermal carrier generation over a wide range of temperatures. The dark

resistivity of good quality crystalline material is of the order of 10^{12} ohm-cm or higher.The density of the material (6.3g/cm^3) results in a large absorption coefficient.The high values of the atomic numbers of the constituent elements(Hg-80, I-53) result in a very large photoelectric effect since the photoelectric interactions are proportional to Z^5,where Z is the atomic number of the interacting material. Single crystalline HgI_2 has been effectively studied and used in the fabrication of X ray and Gamma ray detectors[1,15]. M.Schieber et al.[16,17] have reported that polycrystalline HgI_2 fabricated by means of physical vapor deposition (PVD) technique have higher sensitivity to radiological X rays which is comparable to the results measured with single crystals of HgI_2 and they also found out that the Electrical properties of the PVD polycrystalline HgI_2 were near to those of single crystalline HgI_2.Thus large area thin film polycrystalline HgI_2 which has a much lower production cost is a prospective candidate for direct X -ray radiology. A challenging and sometimes more controversial issue in mercuric iodide growth is the subject of the stoichiometry [1].The range of composition over which mercuric iodide can exist without a change of phase is denoted by HgI_{2-x},where $0 << |x| << 1, x>0$ for mercury rich compositions and $x<0$ for iodine rich compositions.Stoichiometric mercuric iodide is the term referring to the case of $x = 0$.The term “near stoichiometric” refers to the range of x over which the single phase tetragonal mercuric iodide is stable.Evidence that deviations on both the iodine and mercury rich sides of the stoichiometric compositions were detrimental to nuclear radiation detector performance has been reported by Tadjine et al. [18] and it was concluded that

the 2.00 I:Hg ratio was best. HgI_2 detectors are exclusively biased along the crystallographic c-axis for carrier collection and transport properties do depend on the crystallographic direction [1]. Since no dopants are have been found to lower the resisitivity in HgI_2 ,shallow levels in HgI_2 are either highly compensated or they do not exist at all.Therefore deep levels are important in affecting the performance of HgI_2 nuclear spectrometers. R.B James et al. [19] studied the nature and origin of deep level traps in HgI_2 material. They showed that some of the trap types and their concentration was a function of the metal over layer employed as a contact material. Another important issue facing the HgI_2 detectors is the so called polarization effect.The polarization effect is defined as the time dependence of the detector performance that results from the application of the bias field .The effect usually changes the electric field within the device. This thus alters the charge collection efficiency (proportional to the electric field). Possible causes of polarization include trapping, detrapping and change of defect structure in the detector [1].Light spot scanning measurements conducted by Bube [14] on HgI_2 revealed that the photocurrent is mainly limited to a small region at or near the cathode i.e. as the light spot is moved between the cathode and the anode the current is maximum when the spot is near the cathode.This suggests that the photocurrent is mainly due to the contribution from the electrons. Consequently for higher photocurrents the illuminated electrode is negatively biased. The I-V measurements on the HgI_2 -based devices appear often not to be reproducible as the results strongly depend on the experimental procedure. Not only the voltage increment and time left before

increasing the voltage but also conditions of polarization before recording the I-V curves, or the time during which the sample as been left unbiased before the actual measurement also are known to affect the I-V characteristics of the HgI_2 device [20].Surface recombination which also influences the performance of HgI_2 was studied by Levi et al [21] and Z.Burshtein et al. [22].They obtained values for both electron and hole surface recombination velocities in their samples from the Photoconductivity versus Voltage curves .Choice of suitable contact materials to the HgI_2 has always posed a challenge because of the reaction between the contact materials and HgI_2.Silver,Indium and Gallium were all tried but they all reacted with HgI_2 within minutes causing permanent changes to the device[14].When Cu was tried it was found to be devastating to the detector due to Cu diffusion. Palladium, Indium tin Oxide (Transparent conducting oxide), Carbon and Gold have been successfully used as contacts for HgI_2 detectors. With the exception of carbon all of these contacts are deposited either by thermal evaporation or sputtering .Palladium contacts are however nowadays widely used due to their better performance relatively and the high quality of detectors that can be fabricated with them [1].

4.2 Crystal Structure

The primitive unit cell of tetragonal HgI_2 is shown in Fig.4.1.The unit cell comprises of two Hg atoms and four I atoms.Thus the unit cell has two molecules of HgI_2.The nearest neighbour Hg-I spacing is 2.78 Å .The crystal has

an inversion symmetry about the midpoint between the two Hg atoms. The I atoms form a cubic close packing of spheres, and the Hg atoms occupy tetrahedral voids such as to form layers of cornered shared HgI_4 tetrahedra where all I-Hg-I and Hg-I-Hg angles are tetrahedral. The lattice constants are a=b=4.361 Å and c= 12.450 Å at room temperature. [1, 23].If one chooses the midpoint between the two Hg atoms as the origin of the coordinate system, the atomic positions of the two Hg atoms are (-a/4,-a/4,-c/4) and (a/4,a/4,c/4) and those of the four I atoms are (-a/4,a/4,-0.111c),(a/4,-a/4,0.111c),(-a/4,a/4,0.389c) and (a/4, -a/4, -0.389c).

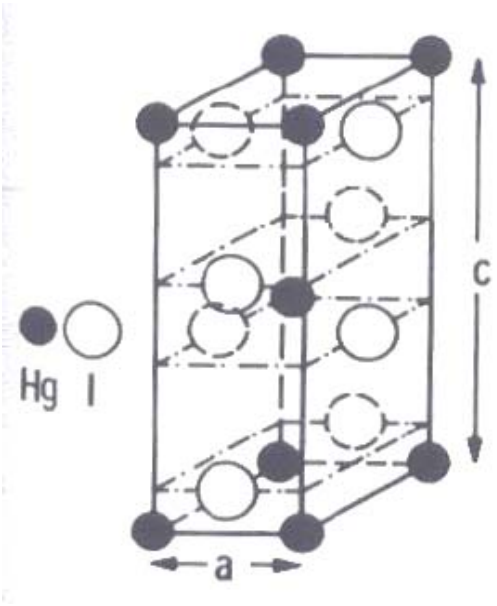

Figure 4.1 Tetragonal Unit Cell of HgI_2 [24]

The Final chapter in this present work discusses the Results and Analysis pertaining to the Optical response of Thin Film Polycrystalline Mercuric Iodide Devices.

CHAPTER 5

RESULTS AND DISCUSSION

5.1 Structure and Layout of the Films

Thin Films of polycrystalline HgI_2 which were analyzed in this work were deposited on a TEC 15 LOF glass substrates coated with a Tin oxide (SnO_2) layer which served as a growth surface and as a front contact to the devices on the film. The deposition technique employed was the Physical Vapor Deposition (PVD).The surface area of deposition had a diameter of about 27mm.The thickness of the films ranged from 132.61μm to 423.63μm.The films showed a preferential (001) orientation such that the c-axis is perpendicular to the substrate. This is also one of the prerequisites to obtaining high quality polycrystalline PVD HgI_2 films [25].Pd contacts were sputtered on to the film through a shadow mask ,with the circular contact area having a diameter of 2mm.Pd contacts function as the back contacts of the devices on the film.Seperate leads were then attached to front and back contacts for the purpose of application of bias.In addition to this a layer of parylene surrounds the HgI_2 film, ensuring the reliability of the films over a long period. It also prevents accidental short circuit between the front and back contacts during measurements.Each Sample is numbered after the date the film on it was fabricated.Each film sample on the substrate consists of seven devices (spots)

with each device comprising of substrate (glass),SnO_2(front contact),HgI_2 film and a Pd back contact. Fig 5.1 (a) shows the layout of the top view of the film Sample and (b) shows the cross-sectional view of the sample.

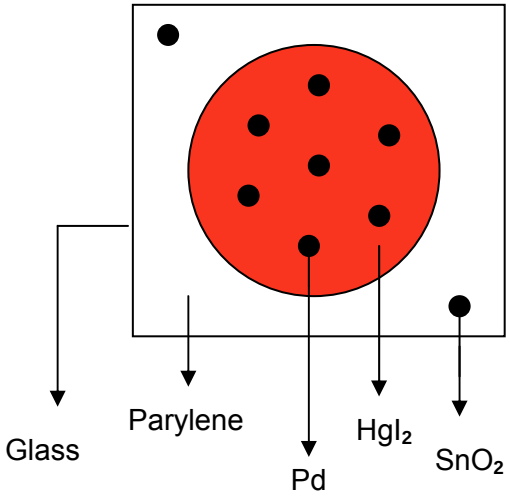

(a)

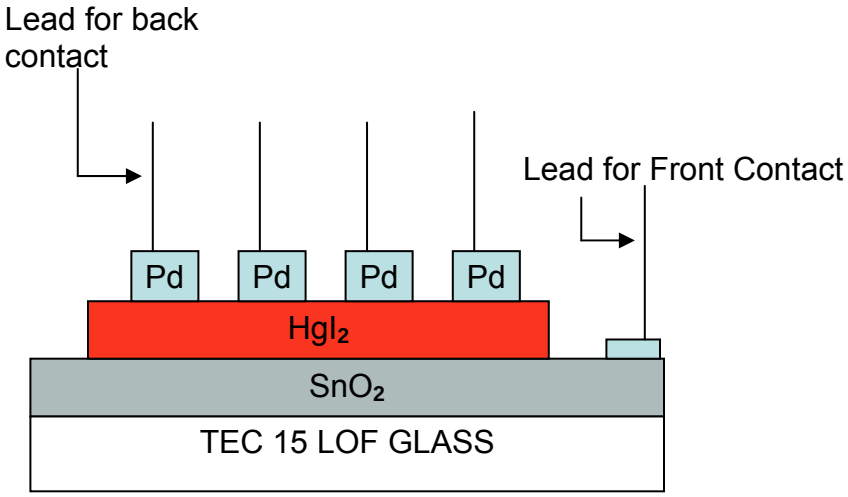

(b)

Figure 5.1 Two Different Views of the Sample

5.2 Experimental Procedure

The Mercuric Iodide Samples were tested for their Spectral response and Current-Voltage (I-V) response in both light and dark conditions.For both these measurements the light source used was a Tungsten- Halogen Lamp.This lamp is a good choice for recording photoconductivity data as its spectral output is in the range 280nm-2500nm [13].Wavelength selection was achieved by means of a Lab View^{tm} data logging program in conjunction with an Oriel grating monochromator.The currents were recorded by using a Keithly 617 programmable Electrometer. Sign of the bias on each device is with respect to the bias applied to the transparent illuminated contact, which is the SnO_2 contact in this case. This contact is termed as the 'Front Contact' and the palladium acts as the 'Back Contact'.It is generally observed that the photocurrent and thus the spectral response is higher when the illuminated contact is negatively biased .This is attributed to the better transport properties of the electrons which traverse the length of the device for this configuration.Therefore the SnO_2 contact is negatively biased and the experimental configuration resembles that shown in Fig. 3.2(a).However currents with positive bias to the front contact were also recorded for comparison purposes. The light from the exit window of the monochromator was focused through the glass substrate (TEC 15 LOF) on a circular area of SnO_2 of 2mm diameter by means of a focusing lens.This circular area was in line with the circular area of the back contact of palladium of diameter 2mm. The Spectral response for each device was obtained at a voltage of -50V applied to the illuminated front contact. For I-V measurements the

voltage was increased from 0V to 50V in steps of 10V and recorded at the peak spectral response wavelength.I-V measurements were carried out in both Light and dark conditions. Because of the possibility of breakdown of the thin films the voltage was not increased beyond 50V.

5.3 Optical Response of the Films

A total of 15 samples were studied in this work .Table 5.1 summarizes the important deposition features of these samples. The total time for deposition is also shown. The films were mostly deposited by the three step process of PVD.In the three step process the substrate was initially maintained at a low temperature then raised to an intermediate temperature and elevated to a final temperature which was maintained until the desired thickness was obtained. The source temperature was also varied during growth.In a modified three step process the substrate temperature is increased from an initial temperature to a final temperature gradually in steps of time. During this increase the source temperature was not changed.In another deposition process called the temperature oscillation process the substrate was oscillated between a low and a high temperature for a number of times.The temperature of the substrate was then maintained at either the low or high temperature to obtain the desired thickness [25].Two films were also fabricated by the two step process of PVD wherein the substrate temperature was maintained at an initial low temperature and finally elevated to a final temperature where it stayed till the desired thickness was obtained.

Table 5.1 Deposition Parameters of the Samples

Sample	T_{SRC} (^oC)	T_{SUB} (^oC)	Thickness (μm)	Type of Process	Total Time (hr)
11-19-02	70, 105	5,35,59	295.55	Three Step	4.5
11-22-02	70, 95	5,35,57	270.34	Three Step	4.5
12-02-02	70,105	5,35,59	423.63	Three step	4.0
12-17-02	70,80	5,…50	213.70	Modified Three Step	5.0
12-19-02	70,80	5,…..53	199.90	Modified Three Step	5.5
01-13-03	70	20,……45	132.61	Modified Three Step	4.5
01-14-03	70	20,……45	149.87	Modified Three Step	5.5
01-15-03	70	20,…….47	152.55	Modified Three Step	5.5
10-09-03	80	Oscillation 5,50	181.33	Temperature Oscillation	2.85
10-20-03	80	30,50	261.71	Two Step	4.5
10-21-03	80	Oscillation 50,30	224.26	Temperature Oscillation	3.5
03-10-04	85	Oscillation 5,50	304.401	Temperature Oscillation	4.0
03-25-04	80	20,…….45	141.532	Modified Three Step	4.5
06-02-04	70	Oscillation 50, 30	266.433	Temperature Oscillation	4.0
09-23-04	90	5,40	350.596	Two Step	3.0

Table 5.2 Peak QE's of the Samples at - 50V Bias to the Illuminated Contact

Sample	Spot # 1	Spot # 2	Spot # 3	Spot # 4	Spot # 5	Spot# 6	Spot # 7
11-19-02	0.209	0.243	0.213	_	0.288	_	_
11-22-02	0.213	0.169	0.174	_	_	0.194	_
12-02-02	0.238	_	0.221	0.247	0.243	_	0.277
12-17-02	0.122	0.179	0.174	_	_	_	0.173
12-19-02	0.206	0.215	0.193	0.114	0.304	0.2931	_
01-13-03	0.132	0.352	0.393	0.315	0.380	0.176	_
01-14-03	0.276	0.266	0.271	0.337	_	0.275	0.234
01-15-03	0.252	0.205	0.131	_	0.228	0.174	0.213
10-09-03	0.190	0.145	0.139	0.134	0.216	_	_
10-20-03	0.171	0.224	0.169	0.247	0.206	0.154	_
10-21-03	0.224	0.128	0.107	0.130	0.161	0.104	_
03-10-04	0.219	0.209	0.209	0.274	0.228	0.313	0.181
03-25-04	0.202	0.262	0.279	0.326	0.321	0.345	0.278
06-02-04	0.167						
09-23-04	0.170	_	0.151	0.119	0.144	0.207	0.240

Table 5.2 lists the Spectral response for the devices on each sample.As seen in the table some of the devices on the samples failed to produce any response.This may be due to a contact failure .Most of the Sample had QE's in the range from 0.1- 0.4.These QE's were recorded at peak wavelengths which ranged from 565nm to 585nm. The absorption coefficient data for the

polycrystalline mercuric iodide is still in the nascent stage.However the data of single crystal mercuric iodide can be used for the present work.This absorption coefficient data is listed in table 5.3 . Some important samples shall now be analyzed with respect to their optical response.

5.3.1 Sample 11-19-02

Fig.5.2 (a) shows the Spectral response of sample # 11-19-02. Five devices (spots) on this sample had efficiency above 0.2.Spot # 5 had the highest efficiency of 0.29 as seen at a wavelength of 565nm. Fig. 5.2 (b) shows the Light I-V curves for this Sample.Dark I-V curves were however very small and could not be recorded .The peak QE of Spot # 5 at 565nm corresponded to a photocurrent of 2.83μA obtained from the data file(see appendix) used to obtain the spectral response for this spot. But the photocurrent from Fig 5.2 (b) reveals a value of 2.34μA. The apparent discrepancy may be due to the time lag in obtaining the I-V curves after the measurement of spectral response. This is observed in all the samples. The measurement of I-V curves with both positive and negative polarity helps to separately study the current due to holes and electrons respectively. With the positive polarity to the illuminated front contact and negative polarity to the back contact, holes are attracted to the back contact. Since the carriers are mainly generated within a distance of few microns from the front surface (Table 5.3), the holes have to travel the greater length of the device

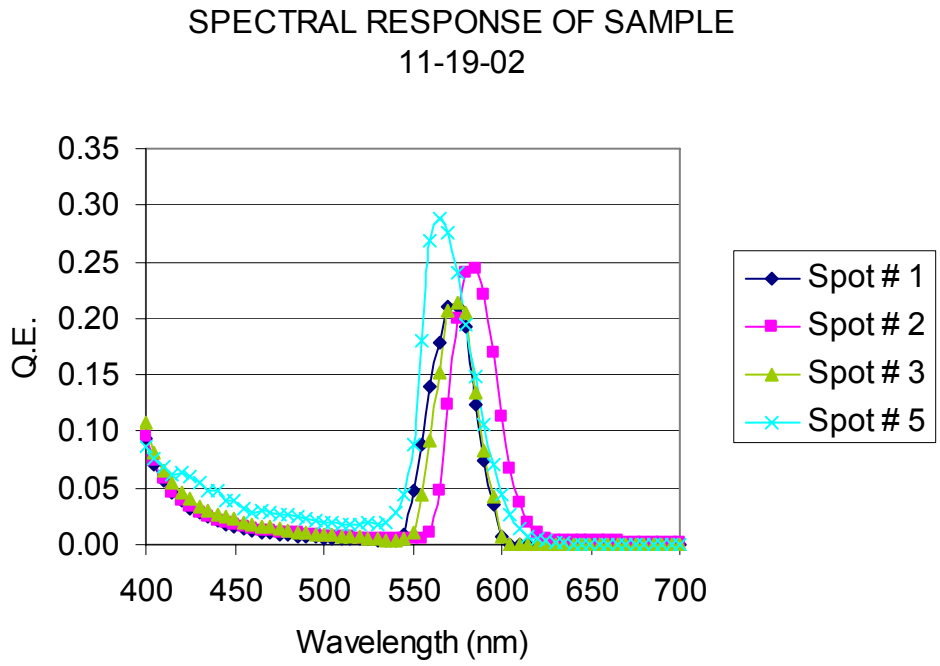

(a)

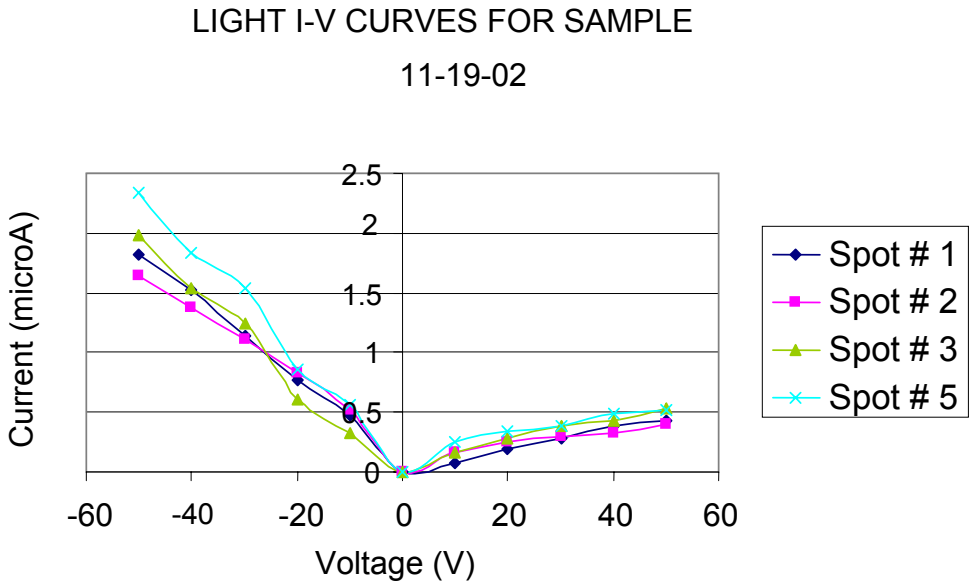

(b)

Figure 5.2 Spectral Response and Light I-V Curves for Sample 11-19-02

Table 5.3 Absorption Coefficient Data [26]

Wavelength (nm)	Absorption Coefficient ,α (cm^{-1})
400	3.2e5
420	2.55e5
440	1.9e5
460	1.5e5
480	1.25e5
500	1.1e5
520	9.0e4
540	7.0e4
560	2e4
580	300
600	11
620	3.5

till they reach the back contact.Therefore the current is mainly due to holes.The reverse is true for negative bias to the front illuminated contact.The current then is mainly due to electrons.As expected the photocurrent with negative bias is higher than that with positive bias as shown in Fig.5.2 (b).This is attributed to better electronic properties of electrons when compared to holes.The holes mainly get trapped or may recombine before they reach the back contact.

A significant feature seen in the spectral response of sample # 11-19-02 and many other samples too is the initial moderate rise in the response at a wavelength of 400nm ,a gradual decrease thereafter with the increase in wavelength,then a sudden increase around the wavelength of about 540nm, observance of a peak around a wavelength of around 580nm and then a rapid fall beyond a wavelength of 595nm(since the absorption coefficient decreases). Attempts to explain the behaviour of the spectral response in the region from 400nm to 550nm and in the region from 550nm to 640nm was carried out by V.Rupavatharam[26],who proposed a two region model to match the measured result with the simulated one.The peak response wavelength roughly corresponds to the minimum energy of a photon (2.1eV) required to excite an e-h pair in HgI_2.

5.3.2 Sample 12-02-02

This sample also had five devices with QE's more than 0.2.The spectral Response and light I-V curves for this sample are shown in Fig. 5.3.The spot # 7 (center spot) had the highest QE of 0.277 at a wavelength of 585nm.This result is a bit surprising because the film on the sample is expected to be thicker at the center and consequently the electric field is expected to be weaker when compared to other spots,leading to lower carrier collection and hence a lower QE.Fig. 5.3(b) shows the photocurrent in the spot # 7 is about 2.184μA at the voltage of -50V to the front contact, obtained at the wavelength of 585nm.The photocurrent for this spot from the Spectral response file is 2.72μA

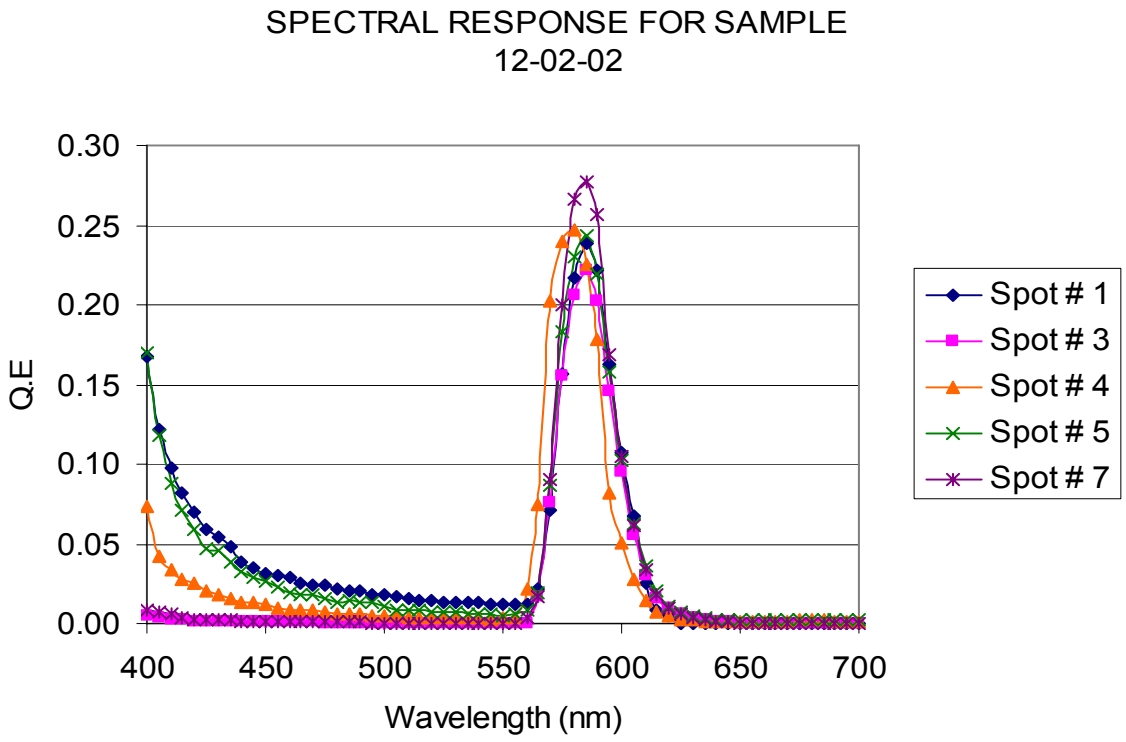

(a)

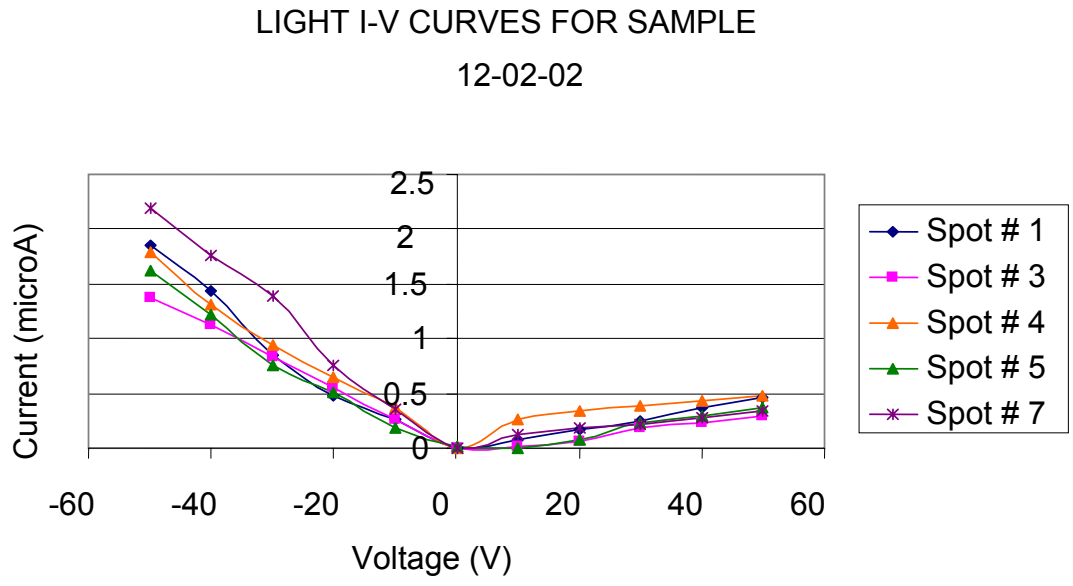

(b)

Figure 5.3 Spectral Response and Light I-V Curves for Sample 12-02-02

and it is this photocurrent that corresponds to the peak QE .The Spectral response reveals that the spot # 3 and spot # 7 had a almost zero response in the region from 400nm to 555nm.Such a behavior is suggestive of the high surface recombination being experienced by the electrons created at the surface.In this sample too the dark currents were very small and could not be recorded.This is actually a good prospect since the dark currents have to be as minimal as possible to achieve good results in these samples.

5.3.3 Sample 01-13-03

This sample had four spots on it whose QE was greater than 0.3.The QE's of the other two spots were low as seen in the Fig .5.4 (a).Comparatively this sample was better than all other samples studied in this work.Also in this sample dark currents in nano Amps range were recorded and are shown in Fig. 5.5.One more feature of this sample is evident in the Spot # 3 of Fig. 5.4 (a).There is a high rise in the spectral response of this sample at the wavelength of 400nm.The photocurrent at this wavelength with a bias of -50V to the front illuminated contact was recorded as 0.2μA from the spectral response data file which was greater than the photocurrent from a spot on a sample which had a almost zero response at 400nm and the same polarity. The current differed by an order of 2.Such a high rise could not be matched even through simulation carried out by V.Rupavatharam [26].Therefore it is to be concluded at this stage

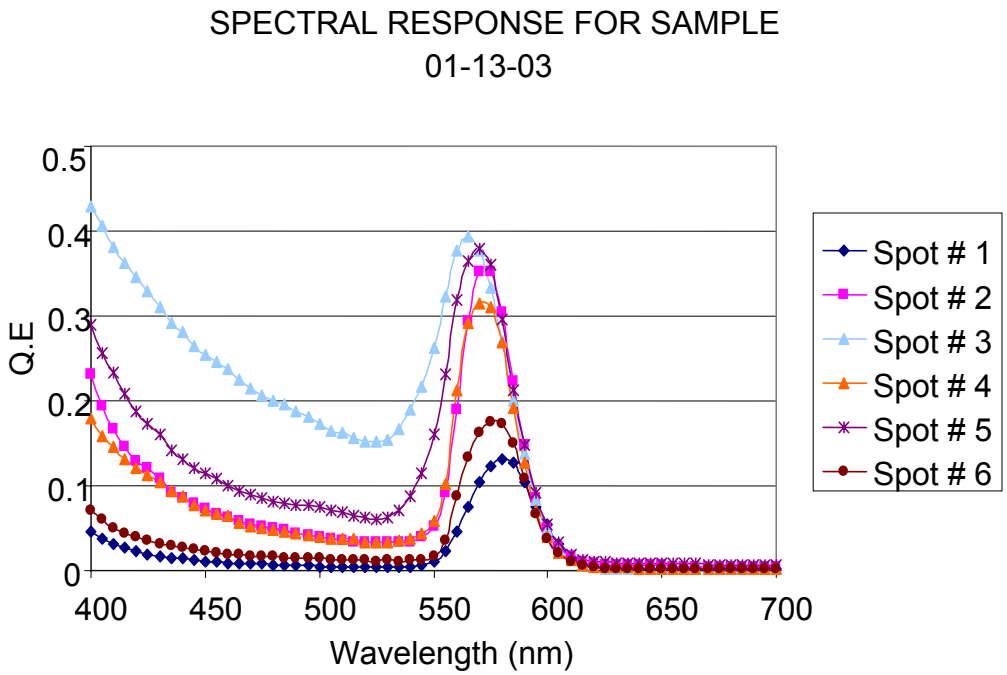

(a)

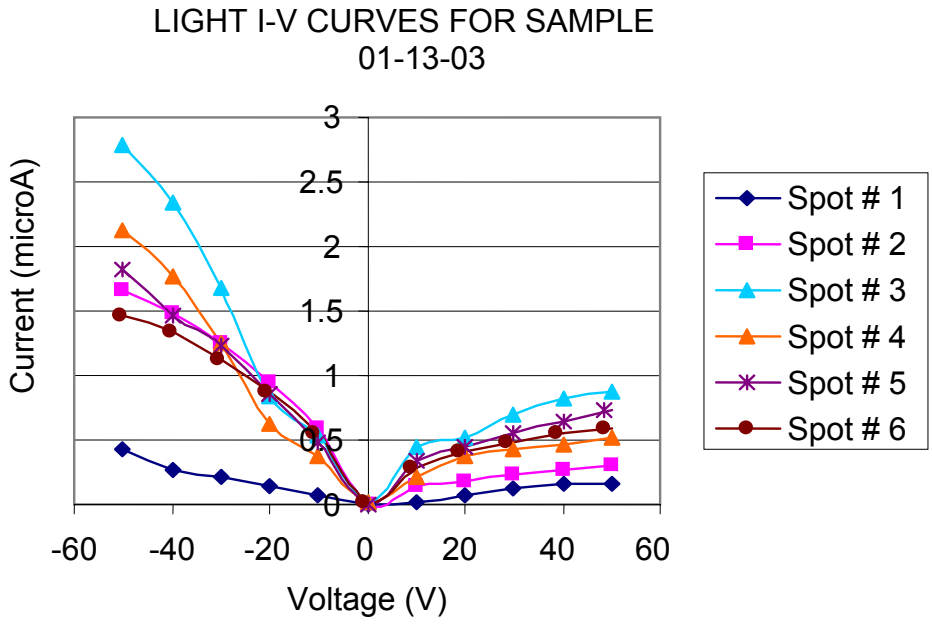

(b)

Figure 5.4 Spectral Response and Light I-V Curves for Sample 01-13-03

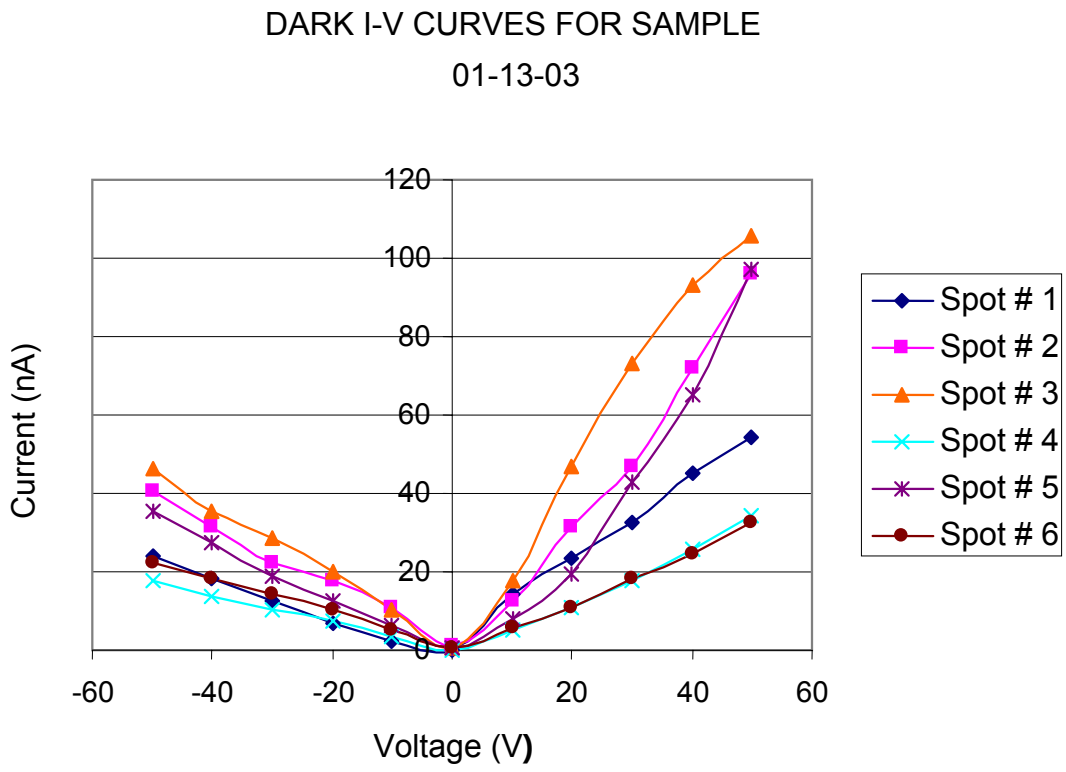

Figure 5.5 Dark I-V Curves for Sample 01-13-03

that such a rise is due to complex electronic processes which usually take place at the surface of such devices [22]. The Spot # 3 had the highest efficiency of 0.39.The photocurrent at a bias of -50V which corresponds to this QE is 3.82μA from the spectral response data file as opposed to the one obtained from the I-V curve of Fig. 5.4 (b) which is 2.8 μA. As expected the dark currents with negative bias are lower than with positive bias shown in Fig.5.5.During the recording of these dark currents it was observed that they changed erratically and were sometimes difficult to tabulate.The shape of these dark currents is indicative of the nature of contacts to each device.If the contacts were symmetric and ohmic ,the dark currents for both polarities would be linearly symmetric on both sides of

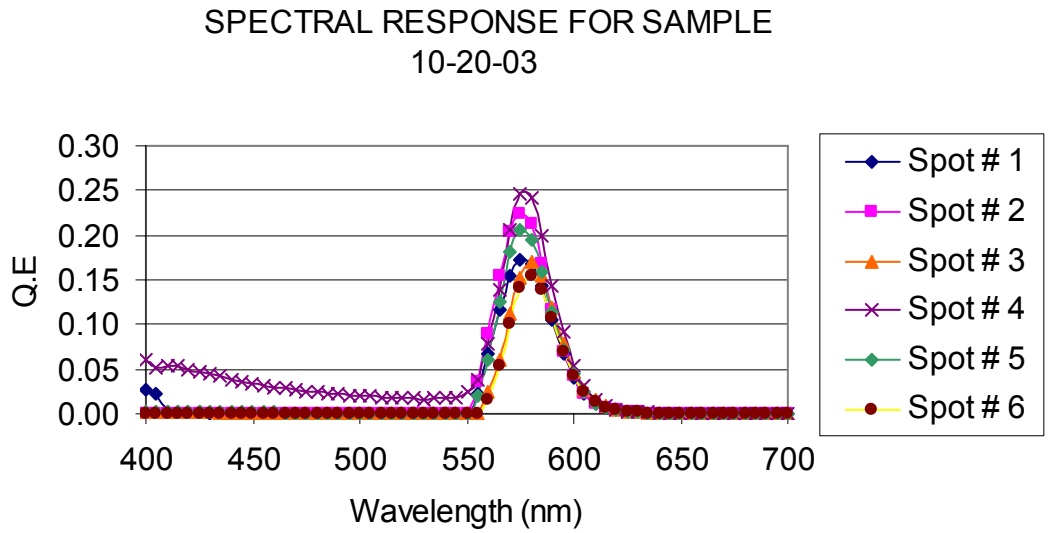

(a)

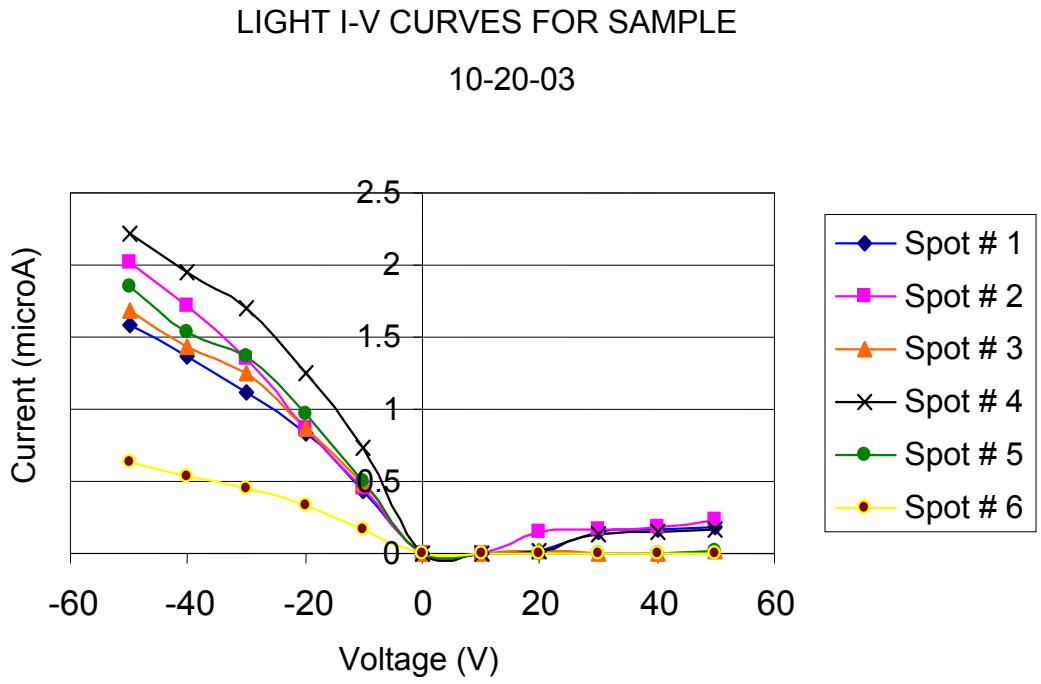

(b)

Figure 5.6 Spectral Response and Light I-V Curves for Sample 10-20-03

the current axis. But this is not the case here. Samples 01-14-03 and 01-15-03 also showed recordable dark currents and their overall response was similar to the one obtained from sample 01-13-03.

5.3.4 Sample 10-20-03

The Spectral response for this sample is shown in Fig.5.6 (a).The devices which showed response on this sample had QE's ranging from 0.17 to 0.25.Spot # 4 has the highest efficiency of 0.25, at a wavelength of 575nm and -50V bias to the front contact.The photocurrent corresponding to this QE for this spot was recorded as 2.61μA from the spectral response file as opposed to the photocurrent recorded from I-V curve of Fig.5.6(b) which is 2.22μA.Also seen from the spectral response for this sample in Fig.5.6(a) is the zero response of all spots except spot # 4 in the region from 400nm to 550nm.The currents in this region were lower by an order of 2 than those obtained for spot # 4.Also from Fig.5.6(b) the I-V curves for the positive bias reveals nearly zero hole currents for 4 spots.This suggests that the prevention of holes from getting collected due to trapping and/or recombination in the bulk. Spots on Sample 10-21-03 and 09-23-04 also showed nearly zero hole currents during illumination.This is shown in Fig 5.7.No dark currents could be recorded for these samples either.

5.3.5 Sample 03-25-04

The spectral response and I-V curves for this sample are shown in Fig 5.8. Spot # 6 on this sample had the highest QE of 0.35 obtained at a wavelength

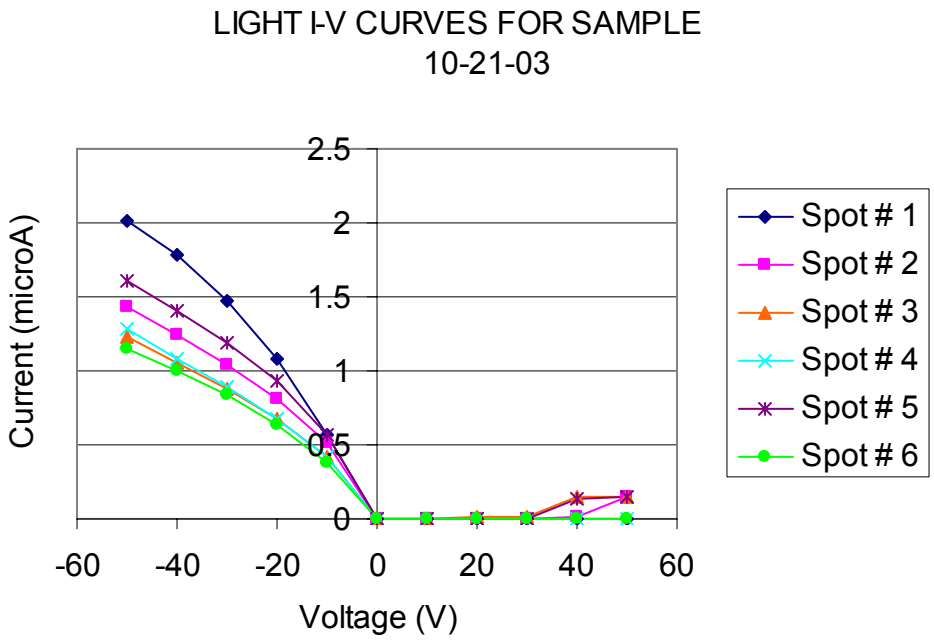

(a)

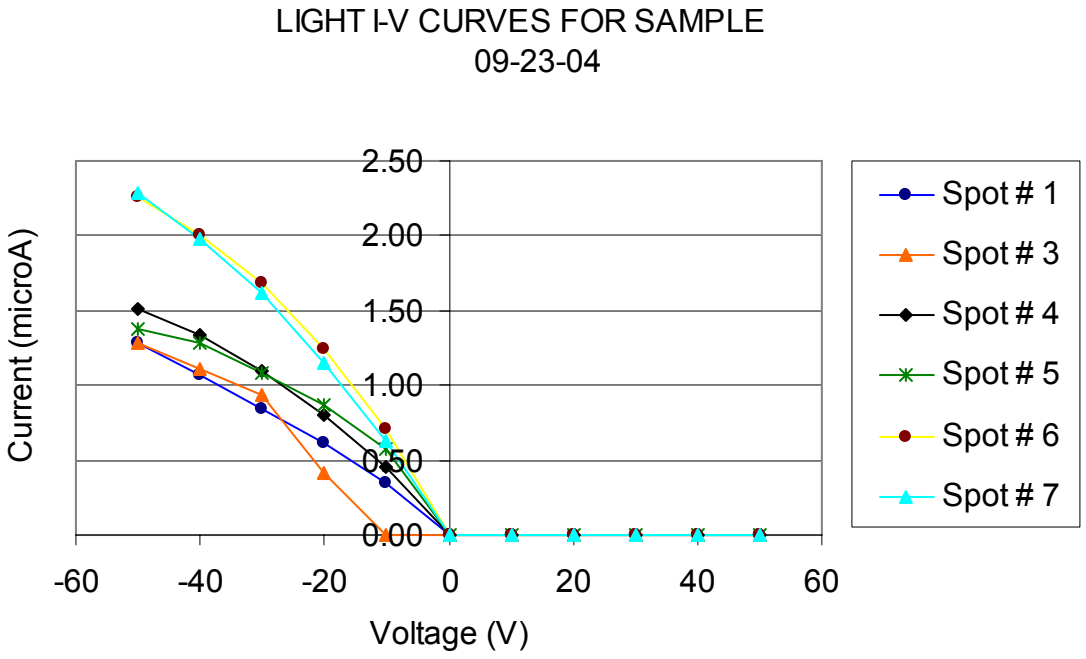

(b)

Figure 5.7 Light I-V Curves for Samples 10-21-03 and 09-23-04

of 565nm and a bias of -50V to the front contact.The photocurrent corresponding to this QE was 3.36μA from spectral response data file as opposed to the value from the I-V curve of Fig .5.8(b) which is 2.74 μA.One significant feature seen in the positive bias region of the I-V curves of this figure is the near saturation of hole currents.This suggests maximum collection has been achieved for the holes and no further increase in hole current is expected with increase in voltage.

Sample 06-02-04 had one spot with a large circular palladium contact. Its QE was measured as 0.17 at a wavelength of 570nm and -50V to the front contact. The photocurrent from spectral response data file was recorded as 1.95μA and that obtained from the Light I-V curve was 1.24μA.No dark currents could be recorded in this sample too.

Many of the results in this work could not be faithfully reproduced and the response of these samples thus depended on initial conditions of voltage,the time for which the sample was left unbiased.This behaviour has also been mentioned in reference [20].

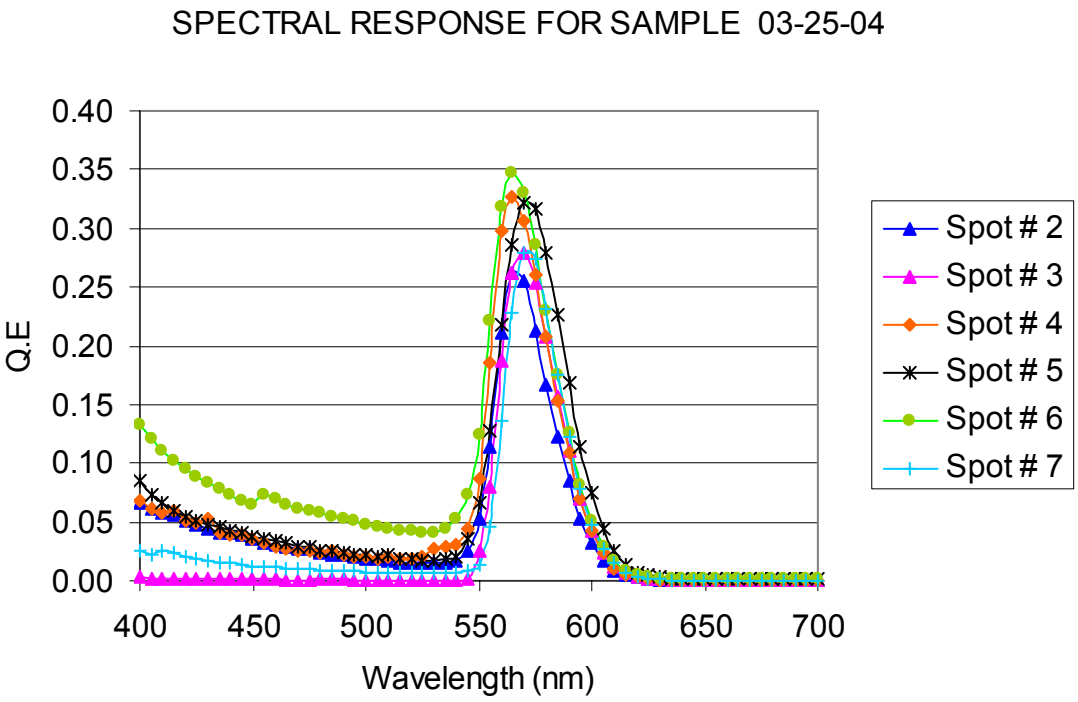

(a)

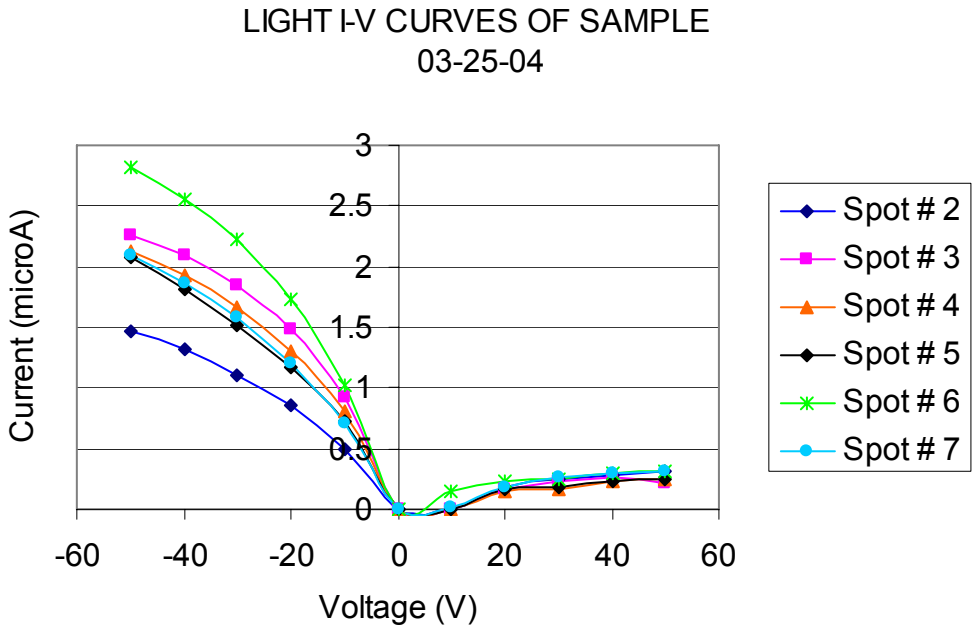

(b)

Fig 5.8 Spectral Response and Light I-V Curves for Sample 03-25-04

CHAPTER 6

CONCLUSIONS

A number of polycrystalline mercuric iodide films were studied as a part of this research.The fabrication conditions of these films which were made by Prince J.Simon [25] have been tabulated in this work.The QE's for the devices on these films with a bias of -50 V to the front illuminated contact have also been presented in this work.The QE's obtained ranged from 0.1 to 0.4.The spectral responses obtained were basically of three types.The first type showed a zero response in the region from 400nm -550nm.This is probably due to high surface recombination for electrons at the surface which prevent them from traversing the device for negative poarity.The second type had a moderate rise in the spectral response at a wavelength of 400nm and then a gradual decrease till a wavelength of 540nm .This was explained on the basis of a two region model simulation carried out in another work on this subject [26].The third type had a high rise at the wavelength of 400nm and a gradual decrease therafter till the wavelength of 540nm.This could not be explained even through simulation and therefore is suggestive of complex electronic processes taking place at the surface.The samples showed a peak response in between the wavelengths from 560nm-585nm which is also affected by absorption. I-V curves were obtained at peak spectral response wavelength in these samples . Most of them had very

low dark currents which could not be recorded. But dark currents could be recorded in three samples viz. 01-13-03,01-14-03 and 01-15-03.The maximum value of dark current value was 77nA with –ve bias to the front contact ,the maximum dark conductivity corresponding to this current was computed as 7.0E-10$(\Omega cm)^{-1}$. Light I-V curves for all samples showed greater response in the negative bias region.This was as expected due to better electronic properties of electrons. But there was apparent small discrepancy in the photocurrents at peak response obtained from spectral response data file and that obtained from I-V curves.This is attributed to the time lag between the spectral response and I-V measurements.The performance of the different films is judged on the basis of consistent high QE's and low dark currents obtained from all the devices on it.On this basis samples 01-13-03 and 03-25-04 proved to be better than the other samples measured in this work.Four devices on sample 01-13-03 had QE's greater than 0.3 This sample also had low measurable dark currents in the negative bias region.Sample 03-25-04 had all its devices giving a response.Three of the devices had QE's greater than 0.3 and three more devices had QE's close to 0.3.The dark currents were also small but not within recordable range.Also both these samples had almost similar fabrication conditions which might have contributed to their better performance.

6.1 Future Work

The surface region of the HgI_2 has been an area of concern in this work.The interpretation of the optical response of this region is a challenging task

which has to be carefully carried out by studying the nature of surface states at the contact -HgI_2 interface.The possibility of the presence of excitons at the surface region has to be investigated through simulation in order to bridge the gap between experimental and simulated results for both the Spectral and I-V responses. . Thermally Stimulated Current (TSC) measurements also have to be carried out on these films to find out the nature of deep traps in HgI_2.

Transient charge techniques such as the Time of Flight (TOF) can be used to evaluate the mobilities of both electrons and holes in these films. Finally the response of these films to X-ray radiation is to be analyzed and compared with the response to Light.

REFERENCES

[1] R.B.James, T.E.Schlesinger, "*Semiconductor and semimetals"*, Vol.43, pp.1-20 and pp.86-216, Academic Press, Inc., (1995).

[2] Harrell G.Chotas, James T.Dobbins III, Carl E. Ravin, *"Principles of Digital Radiography with Large-Area, Electronically Readable Detectors: A Review of the Basics"*, Radiology, Vol. 210, pp.595-599, (1999).

[3] J.S. Iwanczyk et al., *"HgI_2 Polycrystalline Films for Digital X-Ray Imagers"*, IEEE Transactions on Nuclear Science, Vol.49, No.1, February 2002.

[4] G.Zentai et al., *"Large Area Mercuric Iodide X-ray Imager"*, Proceedings of the SPIE, Vol.4682, Medical Imaging, 592, (2002).

[5] Pallab Bhattacharya, *"Semiconductor Optoelectronic Devices"*, Prentice-Hall, Inc.New Jersey, (1994).

[6] Robert F.Pierret, *"Semiconductor Device Fundamentals"*, Addison-Wesley Publishing Company, Inc., (1996).

[7] Richard S.Muller and Theodre I.Kamins, *"Device Electronics for Integrated Circuits"*, Second Edition, John Wiley and Sons Inc., New York, 1986.

[8] S.M.Sze, *"Physics of Semiconductor Devices"*, 2nd Edition, John Wiley and Sons, Inc., New York, (2003).

[9] Richard H.Bube, *"Photoconductivity in Solids"*, John Wiley and Sons, Inc., New York, (1960).

[10] Robert F.Pierret, *"Advanced Semiconductor Fundamentals"*, Second Edition, Pearson Education Inc., New Jersey,(2003).

[11] *http://ece-classweb.uscd.edu:16080/fall04/ece103/lecture5&6&7.pdf* .

[12] Richard H.Bube, *"Electrons in Solids",* Second Edition, Academic Press, Inc., (1988).

[13] N.V.Joshi, *"Photoconductivity"*, Marcel Decker, Inc.,(1990).

[14] Richard H.Bube, *"Opto-Electronic Properties of Mercuric Iodide"*, Physical Review, Vol 106, No.4, pp. 703-717, May 15, (1957).

[15] L.Van den berg et al., *"Mercuric Iodide X-Ray and Gamma Ray Detectors for Astronomy "*, Proceedings of the SPIE, Vol.4497, pp. 100-105, (2002).

[16] M.Schieber et al., *"Near single-crystal electrical properties of polycrystalline HgI_2 produced by physical vapor deposition"*, Proceedings of the IEEE, (2003).

[17] M.Schieber et al., *"Theoretical and experimental sensitivity to X-rays of single and polycrystalline HgI_2 compared with different single-crystal detectors"*, Nuclear Instruments and Methods in Physics Research A,Vol.458,pp. 41-46,(2001).

[18] A.Tajdine et al., *"Search for Correlations between Electrical Characteristics and Stoichiometry in Mercuric Iodide"*, Nuclear Instruments and Methods, Vol.213, pp. 77-82, (1983).

[19] T.E.Schlesinger et al., *"Carrier Traps and Transport in Mercuric Iodide"*, Nuclear Instruments and Methods in Physics Research A, Vol.322, pp.414, (1992).

[20] J.P.Ponpon et al., *"Current Instability in Mercuric Iodide Devices"*, Solid State Electronics, Vol.44, No.1, pp. 29-35, January, (2000).

[21] A. Levi and M.M.Scheiber, *"Carrier surface recombination in HgI_2 photon detectors"*, Journal of Applied Physics, Vol.54, No.5, May, (1983).

[22] Z.Burshtein et al., *"Carrier surface generation and recombination effects in photoconduction HgI_2"*, Journal of Applied Physics, Vol.60, No.9, Nov.1, (1986).

[23] D.E Turner and B.N.Harmon, *"Electronic Structure of Red Mercuric Iodide"*, Physical Review B, Vol.40, No.15, Nov.15, (1989).

[24] S.B.Hyder, *"Trapping effects in silver-doped mercuric iodide crystals"*, Journal of Applied Physics, Vol.48, No1, January, (1977).

[25] Prince J.Simon, *"Polycrystalline Mercuric Iodide Thin Films for Digital Radiation Detectors"*, Master's Thesis, USF (2004).

[26] Vikram Rupavatharam , *"Modelling of QE ,I-V characteristics of MSM (Metal –Semiconductor-Metal)mercuric iodide thin films with MEDICI™ "* Master's Thesis, USF (2004).

APPENDICES

Appendix A Spectral Response Data File

The spectral response curve for each device (spot) on a sample was plotted from the QE data obtained from a file similar to the one shown in Table A.1 on page 66.A part of the data file is shown till the wavelength of 595nm. The second column of the table shows the photocurrent response from the device (spot) on a sample for each wavelength.The QE of the device was found out from the photoresponse from a Si photodiode which was subjected to the same photon flux to which the device was subjected.The third and fourth column of the table therefore shows photodiode photocurrent and its QE respectively. The fifth column shows the QE of the device which can be found out from the relation as follows.

Since the detection of each e-h pair(both the carriers reaching their respective electrodes) contributes to flow one electron worth of current in the external circuit and since the photon flux (number of photons/sec) on the device is the same as that on the photodiode for each wavelength,

$$\text{QE of the device} = \frac{\text{Number of e-h pairs created and detected in the device per second}}{\text{Number of photons impinging on the device per second}}$$

$$= \frac{\text{Number of electrons of current in external circuit of the device per second}}{\text{Number of photons impinging on the device per}}$$

$$= \frac{\text{(QE of photodiode)}}{\text{Photocurrent from photodiode}} \times \text{photocurrent from Device}$$

Appendix A (Continued)

Table A.1 Spectral Response Data File

Wavelength (nm)	Device Response (A)	Si Photodiode Response (A)	Si Photodiode QE	QE of Device
400.01199	6.20E-08	3.95E-07	0.5517	8.66E-02
404.98499	6.69E-08	4.93E-07	0.5556	7.54E-02
409.98999	7.30E-08	6.01E-07	0.5625	6.82E-02
414.992	7.73E-08	7.21E-07	0.569	6.10E-02
419.98901	9.24E-08	8.40E-07	0.5781	6.36E-02
425.01801	1.00E-07	9.70E-07	0.5803	5.98E-02
430.00699	1.03E-07	1.10E-06	0.585	5.49E-02
434.991	1.01E-07	1.26E-06	0.5866	4.74E-02
440.008	1.12E-07	1.41E-06	0.588	4.69E-02
444.983	1.05E-07	1.57E-06	0.5913	3.94E-02
449.991	1.13E-07	1.74E-06	0.5943	3.85E-02
454.99399	1.04E-07	1.92E-06	0.5974	3.22E-02
459.992	1.01E-07	2.11E-06	0.6008	2.86E-02
464.98599	1.12E-07	2.30E-06	0.603	2.92E-02
470.01099	1.18E-07	2.51E-06	0.6053	2.85E-02
474.995	1.21E-07	2.71E-06	0.6075	2.71E-02
480.01099	1.24E-07	2.93E-06	0.6097	2.57E-02
484.98599	1.23E-07	3.15E-06	0.612	2.39E-02
489.991	1.27E-07	3.37E-06	0.6143	2.31E-02
494.992	1.21E-07	3.61E-06	0.6167	2.06E-02
499.98801	1.24E-07	3.87E-06	0.6188	1.98E-02
505.01401	1.29E-07	4.13E-06	0.62	1.94E-02
509.99899	1.31E-07	4.40E-06	0.6183	1.84E-02
515.01502	1.34E-07	4.63E-06	0.6196	1.79E-02
519.98999	1.44E-07	4.90E-06	0.6234	1.83E-02
524.995	1.53E-07	5.13E-06	0.6288	1.87E-02
529.995	1.55E-07	5.38E-06	0.6216	1.79E-02
534.98901	1.74E-07	5.58E-06	0.6267	1.95E-02
540.013	2.55E-07	5.79E-06	0.6263	2.76E-02
544.99597	4.26E-07	6.01E-06	0.6269	4.44E-02
550.00897	8.89E-07	6.28E-06	0.6282	8.89E-02
555.01703	1.88E-06	6.55E-06	0.6277	1.80E-01
560.01801	2.87E-06	6.82E-06	0.6384	2.69E-01
565.013	3.25E-06	7.11E-06	0.6315	2.88E-01
570.00201	3.23E-06	7.41E-06	0.6319	2.76E-01
574.98602	2.92E-06	7.66E-06	0.6335	2.41E-01
579.99799	2.43E-06	7.89E-06	0.6327	1.94E-01
585.00501	1.90E-06	8.07E-06	0.6327	1.49E-01
590.00501	1.38E-06	8.22E-06	0.6339	1.06E-01
594.9902	8.80E-07	8.48E-06	0.6367	6.61E-02